THE EFFECTS OF WATER ON THE PHYSICAL PROPERTIES OF SILICA AEROGELS

By

Shira G. Mandel

****

Submitted in partial fulfillment
of the requirements for
Honors in the Departments of Mechanical Engineering and Chemistry

UNION COLLEGE
June, 2005

ABSTRACT

MANDEL, SHIRA The Effects of Water on the Physical Properties of Silica Aerogels. Departments of Mechanical Engineering and Chemistry, June 2005.

Aerogels are polymers, intricate networks of macromolecules chemically woven together. The nanostructure is 90-99 % air, making aerogels the lightest solid known to man. (Bakrania, 2002; Stardust, 1999) Other unique properties of the aerogel include their exceptional insulating abilities, as well as low thermal, electrical and acoustical conductivities. (Brinker and Scherer, 1990)

The research found in this report focuses on varying the amount of water used in the fabrication of silica aerogels and characterizing the effect this has on their physical properties, such as density, thermal conductivity and transmittance. So far, the aerogels made with the "original" recipe have produced average density of 0.09 g/cm^3 and thermal conductivity of 0.04 W/mK; these properties are not significantly altered as the amount of water used is increased or decreased. However, there is an observable trend in transmittance; as more water is added to the "standard" recipe, the resulting monoliths become more transparent and less opaque indicating that more light is transmitted through the samples.

Also included in this report is a study of aerogels as potential platforms for chemical sensors. We have successfully entrapped the luminescent probe, platinum (II) octaethyl porphyrin (PtOEP), in several aerogel samples utilizing Union's rapid supercritical extraction process. The fluorescence of PtOEP is quenched in the presence of oxygen. Spectral characterization shows that as the amount of water used to fabricate

the PtOEP-doped aerogels increased, the ratio of fluorescence intensity in 100% N_2 to that in the presence of air (ca. 21.5% O_2) decreased.

ACKNOWLEDGEMENTS

First and foremost I would like to acknowledge my advisors. I would like to thank Professor Ann Anderson for bringing me into the world of aerogels. She has always provided advice and enthusiasm throughout this project. I would also like to thank Professor Mary Carroll for her support throughout the years and her continuous guidance, particularly during the writing process.

I would like to acknowledge my fellow students on the Aerogel Team. I have enjoyed working with Liz Lax and Melissa Passarelli in the lab throughout this year, sharing data, ideas and problems.

I must also acknowledge past students such as Ben Gauthier'02 who developed the fabrication technique used to make our aerogels, and Smitesh Bakrania '03 for the graphics and illustrations I use in all of my presentations.

I would like to thank Jim Howard and Roland Pierson in the Machine Shop for the manufacturing of our aerogel molds.

Lastly, I must thank the NSF-MRI Program for the AFCAL research lab and equipment, as well as Union's Intellectual Enrichment Grant for the financial support of my senior research project.

TABLE OF CONTENTS

1 PROJECT OBJECTIVE 1

2 BACKGROUND 2

2.1 Introduction to Aerogels 2
2.2 Fabrication of Aerogels 2
2.3 Aerogels as Platforms for Chemical Sensors 4
2.4 Literature Review 6
2.4.1 Effects of Chemical Precursors on the Physical Properties of Aerogels 6
2.4.2 Effects of Water Content on the Density and Transmittance of Aerogels 7
2.4.3 Using PtOEP-Doped Polymers for Gas Sensor Applications 10

3 EQUIPMENT AND PROCEDURES 12

3.1 Materials 12
3.2 Fabrication 12
3.3 Density Calculations 13
3.4 Thermal Conductivity Measurements 14
3.5 Transmittance Measurements 16
3.6 Fluorescence Measurements 17
3.6.1 Emission Scans 18
3.6.2 Time-Based Scans 18

4 DATA ANALYSIS AND RESULTS 19

4.1 Density 20
4.2 Thermal Conductivity 24
4.3 Transmittance 25
4.4 Fluorescence of PtOEP-Doped Aerogels 31

5 DISCUSSION OF RESULTS 36

5.1 Density 36
5.2 Thermal Conductivity 38
5.3 Transmittance 40
5.4 Fluorescence Study 42

6 CONCLUSIONS AND FUTURE WORK 45

7 REFERENCES 48

8 APPENDICES 50

8.1 Appendix A: "Standard" Recipe 50
8.2 Appendix B: Solidworks Mold 51
8.3 Appendix C: Hot Press Setup 53
8.4 Appendix D: Solidworks Aerogel Sample Holder for Reflectometer 54
8.5 Appendix E: Hot Disk Analyzer Set-Up and Measurement Procedure 56
8.6 Appendix F: Reflectometer Set-Up and Measurement Procedure 59
8.7 Appendix G: Fluorometer Set-Up and Measurement Procedure 61
8.8 Appendix H: Emission Spectra of PtOEP-Doped Aerogels in 100% Nitrogen 63
8.9 Appendix I: $F_{(100\% N2)}/F_{(Air)}$ for Each PtOEP-Doped Aerogel 71
8.10 Appendix J: Time-Based Scans of PtOEP-Doped Aerogels 72

1 Project Objective

Previous research in the Aerogel Fabrication, Characterization, and Applications Lab (AFCAL) at Union College has focused on the fabrication techniques and properties of silica-based aerogels, which have silicon-oxygen matrices. The effects of the individual chemical precursors on the physical properties of the aerogels have not been investigated. The objective of this research project is to explore the effects of the proportions of water used in the aerogel fabrication process on the physical properties of the resulting silica-based aerogels. This will be accomplished by characterizing the density, thermal conductivity, and transmittance of the aerogels.

Aerogels also have the potential to be used as solid hosts of sensor probes due to their large amount of surface area and solid matrix structure. Therefore, this research project will also focus on the applicability of these materials as platforms for optical sensors. Specifically, it explores how the proportions of water used in the chemical precursor mixture affect the response of an entrapped luminescent probe, PtOEP, to oxygen; thus, the aerogels' suitability as a platform for this gas sensor.

2 Background

2.1 Introduction to Aerogels

Aerogels are polymers, intricate networks of macromolecules chemically woven together. The fabrication of this material includes a polymerization reaction followed by solvent evacuation, which produces a nanostructure that is 90-99 % air, making aerogels 1,000 times less dense than glass, yet almost 39 times more insulating. (Bakrania, 2002; Stardust, 1999) Other unique properties of the aerogel include an extremely low index of refraction as well as low thermal, electrical and acoustical conductivities. (Brinker and Scherer, 1990)

2.2 Fabrication of Aerogels

The first step in the fabrication of an aerogel is a chemical reaction; specifically, a polymerization process to form a sol-gel. The process begins by hydrolyzing a precursor chemical using an acid or base catalyst. The most commonly used reagents are metal alkoxides hydrolyzed by water. The particular alkoxide chosen will determine the composition of the sol-gel polymer network. The polymerization process starts with condensation followed by poly-condensation to form a "wet" gel, which consists of a cross-linked polymer suspended in a solvent, determined by the reagents used in the initial chemical reaction.

After initiating the polymerization reaction by mixing the chosen precursors, the chemical process proceeds until the liquid solution forms a wet gel structure that consists of the solid polymer matrix submersed in a solvent. The solvent in the sol-gel must then be evacuated and replaced with air to produce an aerogel. This portion of the process can

be done using ambient pressure techniques (to form films and powders) or supercritical extraction techniques (to form monoliths).

If the solvent in a sol-gel were to evaporate naturally, a xerogel would be produced. As the solvent evaporates, it exerts capillary forces on the polymer, which can collapse the fragile nanostructure. A xerogel will shrink to one eighth its original size and the material will be denser than an aerogel as it is only 60-90% air. (Brinker and Scherer, 1990) Specific solvent evacuation techniques are necessary to prevent the nanostructure of the sol-gel from collapsing, and therefore increasing the density of the final material, in order to produce an aerogel.

The conventional supercritical extraction technique reduces surface tension in the sol-gel by bringing it to the solvent's critical point, so that it can be evacuated without collapsing the polymer structure. (Kistler, 1932; Gauthier, 2004) First, the chemical precursors are mixed and allowed to form a wet gel. Then, before the gel is dry, it is taken through a solvent-exchange process. The methanol within the gel is replaced with CO_2 during this process because methanol's critical point is at a much higher pressure and temperature; the critical point of CO_2 is much easier to reach with conventional methods. After the exchange, conditions above the supercritical temperature and pressure are obtained for the CO_2 utilizing an autoclave and the supercritical fluid is extracted from the solid matrix. This process that includes gelation, solvent exchange and supercritical extraction to produce the final aerogel can take as a long as two weeks.

A new production method, recently developed at Union, uses rapid supercritical extraction. (Poco et al., 1996; Gauthier, 2004) The polymerization reagents and catalysts are poured directly into a mold, which is heated rapidly by a hydraulic hot press. The

heating of the platens increases the temperature of and the pressure on the chemical solution inside the mold as the liquid solution starts to expand to a gas. Utilizing a hot press enables the solution to reach a high enough temperature and pressure for all of the solvent (methanol and water mixture) to be in the supercritical phase; therefore, the exchange procedure, which replaces the alcohol with liquid CO_2, is unnecessary. When the supercritical point of the solvent is reached, the restraining forces from the hot press are released, allowing the supercritical gases to escape. Compared to the conventional method described above, this technique can be completed in much less time, approximately seven hours and in only one step. (Gauthier, 2004)

2.3 Aerogels as Platforms for Chemical Sensors

One of the potential applications for the aerogel is to use it as a platform for a chemical sensor. Chemical sensors are usually complex molecules that have some type of response to a particular change in their environment. These molecules can be hosted by a solid substance, physically entrapped or chemically bonded to the matrix of a film or monolith, (Lu et al., 2001, Leventis et al., 1999) or they can be suspended in a solution.

There are many important uses for chemical sensors. They can be used to detect harmful changes in their environment for health and safety awareness, military purposes, or even environmental concerns, among other uses. For a sensor to be useful it is best if its response is fast and it is significant enough to be easily detected and quantified. In addition, the most practical sensor would also be reversible and its response should be repeatable so it can be used more than once. Depending on the accuracy and precision necessary for its purpose, it should be able to respond to a small quantity of analyte. (Plata et al., 2004)

For this investigation, in particular, aerogels were used as platforms for gas sensors. Gas sensors are chemical sensors that respond to certain types of gas-phase substances in their environment. Aerogels have the potential to be ideal platforms for these types of sensors for the following reasons: first, their solid structure offers a stable support for the chemical probes; second, aerogels can be optically transparent and can therefore be useful for hosting optical sensors; third, the probe can be entrapped in the aerogel matrix through physical interactions rather than a covalent bonding, which makes the doping process easier; fourth, analyte species that are small are able to permeate the aerogel matrix quickly to interact with the chemical probes; and lastly, the material has a very large amount of surface area, which will enable the gaseous analyte to access the sensor easily as there are many points of interaction within the matrix.

One disadvantage to the use of aerogels as platforms for chemical sensors is that the fabrication process usually applies high temperatures to the chemical precursor mixture. This prohibits the use of thermally unstable chemical probes, as they will decompose under such high temperature conditions during the fabrication process.

The chemical sensor of focus in this investigation was a platinum (II) octaethyl porphyrin (PtOEP). Its structure is shown in Figure 1. PtOEP is a fluorescent complex that emits light at approximately 646 nanometers when excited in the visible region, at approximately 533 nm. The fluorescence of PtOEP, however, is quenched in the presence of oxygen as a result of the binding of O_2 to

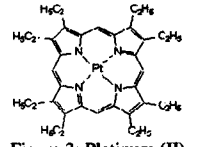

Figure 3: Platinum (II) Octaethyl Porphyrin (PtOEP) (www.chemfinder.com)

the center platinum element. This property of the molecule makes it a potential gas sensor for oxygen.

Metalloporphyrin oxygen sensors, such as PtOEP, are commonly used for gas sensing applications for several reasons, including the fact that they are excited by light in the visible region (533 nm) and they exhibit high sensitivity (Lee and Okura, 1997). When PtOEP is used in a polymer matrix, however, its function as a sensor will depend on the properties of its host structure. Therefore, it is best to use it in conjunction with a polymer that has a high diffusion rate for oxygen if it is to be used as a gas sensor (Amao et al., 2000). It is for this reason that aerogels are promising materials as platforms for this luminescent probe.

2.4 Literature Review

2.4.1 Effects of Chemical Precursors on the Physical Properties of Aerogels

The chemical precursors used are an extremely important aspect of the overall fabrication of aerogels. Changing the amount or structure of any of the chemicals can alter the physical properties of the resulting aerogels. Currently, in AFCAL, TMOS is used to initiate the polymerization of a silicon-oxygen matrix because it is a silica-based chemical. If an alumina-based chemical is used to replace TMOS, the aerogel matrix will be an aluminum oxide. One could also replace TMOS with a slightly different silica based material known as TEOS and presumably alter the structure of the silicon-oxygen matrix. Wagh et al. (1999) studied these two precursors and found that transmission decreased when using TEOS as opposed to TMOS and that the pores in the aerogels were non-uniform instead of narrow and uniform.

The physical properties of aerogels can also be influenced by changing the type of solvent (an alcohol) or catalyst, or by changing the amount of water involved in the preliminary chemical reaction. Rao et al. (1994) researched the effect of chemical precursors on the properties of silica aerogels by fabricating aerogels using a variety of alcohols and catalysts. They found that the shorter the chain of the alcohol was, the lower the rate of gelation would be due to steric hindrance, transesterification and hydrogen bonding. In addition, increasing the amount of solvent or water would decrease both the SiO_2 and TMOS concentrations, thereby decreasing the gelation time and density of the final aerogel monolith.

When varying types of catalyst, Rao et al. (1994) found that acid-catalyzed aerogels had smaller pores and experienced greater cracking than base-catalyzed aerogels. The base-catalyzed aerogels tended to have lower densities and were more transparent and monolithic. Rao et al. concluded that acid catalysis, causes the condensation reaction to start at a later stage than basic catalyst. Gelation time was also affected by the type of catalyst used; a strong basic catalyst produced the shortest gelation time whereas aerogels produced with an acidic catalyst took the longest time to gel. It was also apparent that increasing the amount of catalyst would increase the rate of gelation.

2.4.2 Effects of Water Content on the Density and Transmittance of Aerogels

Previous work concerning the effect of water on the physical properties of aerogels has been performed by Rao et al. (1994). Of particular interest are the group's findings on how the amount of water used in the precursor solution affects the density

and percent transmittance of the resulting aerogels. For their investigation, Rao et al. held the molar ratio of the concentration of methanol to the concentration of TMOS at a constant value of 12, while varying the molar ratio of water to TMOS from 2 to 16.

The density of the resulting aerogels ranged from 0.005 g/cm^3 to 0.1 g/cm^3. More specifically, Rao et al.'s results, displayed in Figure 1 show that the lowest-density aerogels are made when the ratio of water to TMOS is between 4 and 6. Starting at a one to one ratio of H_2O to TMOS the density of the aerogels will decrease very quickly until the H_2O/TMOS ratio reaches the previously indicated minimum. Then, as the H_2O/TMOS ratio increases further, the density will start to increase more slowly then it decreased.

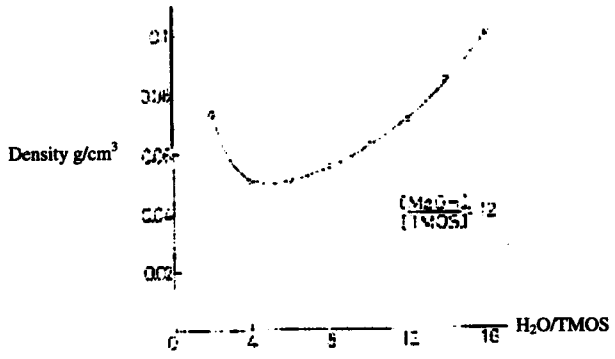

Figure 1: Density of the Aerogel as a Function of Molar Ratio of H_2O/TMOS

(Rao et al., 1994)

The percent transmittance of the Rao et al.'s aerogels displays a different trend. At first, when the ratio of water to TMOS is increased from 2 to 4, the percent transmittance of light at 900 nm increased from 70% to 90% transmittance. (Percent transmittance of light in visible region was not included in their results.) At this point, however, the percent transmittance of the resulting aerogels seems to stop changing and levels off at 90% transmittance as the ratio was increased further. Figure 2 shows this trend; note that changes in molar ratios of water to TMOS higher than 4 do not seem to affect the percent transmittance of the aerogel samples. (Rao et al., 1994)

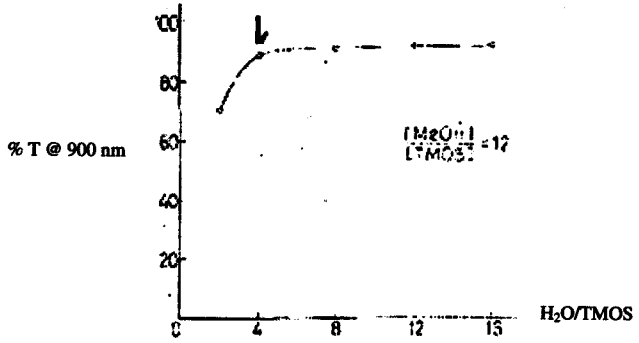

Figure 2: Percent Transmission of the Aerogel as a Function of Molar Ratio of H_2O/TMOS at 900 nm with 1 cm thick aerogel (Rao et al., 1994)

2.4.3 Using PtOEP-Doped Polymers for Gas Sensor Applications

The luminescent probe PtOEP has the potential to be used as a gas sensor because its fluorescence is quenched by oxygen. It is for this reason that scientists have been investigating the properties of this probe in silica matrices. Amao et al. (2000) embedded the porphyrin in a silica-based film to study its performance as an optical sensor for trace amounts of oxygen. They saw PtOEP absorption maxima at 534, 501, and 378 nm and an emission maximum at 646 nm. The poly[1-(trimethylsilyl)-1-propyne] (poly[TMSP]) films were found to be highly gas permeable, therefore producing a very low oxygen sensing limit of less than 0.3% and a sensitivity ratio, I_0/I_{100} (fluorescence intensity in 100% argon to 100% oxygen) of approximately 225. The Stern-Volmer equation was found to be $I_0/I = 1 + 5.7\%^{-1}[O_2]$. Amao et al. found that these films had a very fast response time of 3.6 seconds when starting the films in argon and introducing oxygen; however, this increased when going the opposite direction from oxygen to argon with a response time of approximately 73.2 seconds.

Lee and Okura (1997) investigated PtOEP-doped silica-based sol-gel films made from TEOS as oxygen sensors. This group saw PtOEP absorbing at 536, 502, and 380 nm and emitting light at 646 nm. The sol-gel films produced stable signals that were reversible and reproducible. As in the work of Amao et al., they observed fast response times for their PtOEP doped films; starting in 100% nitrogen and going to 100% oxygen the response time was 5 seconds, whereas it was 10 seconds in the opposite direction. Lee and Okura also found that the transparency, color, sensitivity and Stern-Volmer linearity were affected by the temperature used to dry the films, which they attributed to a

change in the structure of the porous matrix and the microenvironment of the entrapped luminescent probe.

3 Equipment and Procedures

3.1 Materials

Tetramethyl orthosilicate (TMOS) was purchased from Sigma-Aldrich at 98% purity. A previously prepared saturated solution (concentration less than 2.0×10^{-4} M) of PtOEP dissolved in methanol was used to fabricate PtOEP- doped aerogels. The PtOEP was purchased from Frontier Scientific. The 1.5 M ammonium hydroxide catalyst solution was prepared from a 99.99% pure stock purchased from Sigma-Aldrich. Kapton, graphite sheets, and aluminum foil were used as gasket material for the hot press procedure. The Kapton was purchased from American Durafilm, the graphite sheets were purchased from Phelps Industrial Products and Reynolds Wrap aluminum foil was purchased from a local grocery store. The aerogel mold was machined in-house from 1018 cold-rolled steel. DEM-KOTE T.F.E. Dry Lube teflon spray (2W757B, non-chlorinated) was used to coat the inside of the mold before each use.

3.2 Fabrication

To begin the fabrication process, the chemical precursors were measured using a Maxipettor for the water, methanol and TMOS and a 100-1000 μL pipet for the ammonium hydroxide catalyst, in the appropriate proportions (see Appendix A: "Standard" recipe). To fabricate PtOEP-doped aerogels, we simply replaced the amount of methanol in the recipe with the same amount of a solution of PtOEP dissolved in methanol (concentration less than 2.0×10^{-4} moles/liter). The 9-hole, steel mold (see Appendix B: SolidWorks Mold) was washed, sanded, and sprayed with a non-stick Teflon coating. It was then placed on top of a "sandwich" of aluminum foil, graphite

gasket material, and kapton in the hot press (see Appendix C: Hot Press Setup). The empty mold was then secured in the hot press by applying 500 psi of pressure on it by the platens in the manual mode and initiating the program by simultaneously pressing the two black close buttons. When both the solution and mold were ready, the hot press was opened and the chemical precursor mixture was transferred to the mold with a glass pipet, filling each hole completely. Another layer of kapton, gasket material and aluminum foil were then placed on top of the mold, in that order, and the hot press was switched to automatic mode.

The hot press was used to fabricate aerogels by controlling the temperature and pressure of the two platens. A sequence of varying pressure and temperature with respect to time was programmed into the memory using the automatic mode, which was saved for future runs. After the pre-programmed pressure-temperature sequence was entered and checked (see Appendix C: Hot Press Setup), it was initiated by simultaneously pressing the two black close buttons. When the fabrication was complete the aerogels were taken out of the mold, stored in boxes, and labeled with the date fabricated and their position in the mold with respect to the hot press. (See Figure 7 in Density Results Section.)

3.3 Density Calculations

The aerogel samples from AFCAL were fabricated in cylindrical shapes. This simplified density calculations for the monoliths significantly. A caliper was used to measure the height, H, and the diameter, D, of each aerogel sample to the nearest 0.001 inches. From these measurements, we calculate the volume of the aerogel cylinder: Volume = $(H\pi D^2)/4$. An OHAUS Explorer balance was used to measure the mass to the

nearest 0.0001 grams. An estimate of the sample's density was then found dividing mass by the volume. It was important to convert the units of volume into cubic centimeters in order to compare results with the literature, as the standard units of density are in g/cm^3.

3.4 Thermal Conductivity Measurements

Thermal conductivity measurements were performed using the Hot Disk Thermal Constants Analyzer system, version 5.7 (copyright Hot Disk Inc. and Thermetrol Inc.). The components of the thermal analyzer system include the sample holder and sensor, the bridge, a Keithley source meter and multimeter, a computer, and a separate computation unit.

There are two types of tests that can be performed with the Hot Disk Thermal Analyzer: one-sided tests where the sensor is "sandwiched" in between the sample and a standard background material of known conductivity, and two-sided tests where the sensor is sandwiched in between two pieces of a sample. For the one-sided test it is required that the standard background material be more insulating than the sample being tested. Because aerogels are highly insulating, it is unlikely that there is a suitable material for use as the background standard and therefore, only two-sided tests were performed in this research investigation. (See Appendix E: Hot Disk Analyzer Set-Up and Measurement Procedure.)

A sample used in the thermal conductivity analysis had to have a diameter that was twice the size of the sensor diameter and a thickness that was at least the size of the sensor diameter both above and below the sensor. These restrictions are set so that the spherical release of heat, created by the sensor, is not affected by the edges of the sample, as the calculation assumes that the sensor has been placed in an infinite medium. The size

of the sensor used in this experiment was the C5465, 3.189 mm (~0.126 inch diameter) sensor, so the aerogel samples had to be at least 0.25 inch in diameter and in height, in order to perform the two-sided test. The surface on which the sensor is placed must also be flat and smooth, as though the sensor were imbedded within the sample. The aerogel samples used in this experiment were made in 0.83-inch diameter, 0.75-inch deep molds. They were extremely fragile and not easily sliced in half while maintaining two smooth surfaces without breaking. For an ideal two-sided test, the sample must break along a smooth surface, close to the center of the sample. However, most of the time, the aerogel samples did not break in this manner and two different samples had to be used for a single two-sided test. In this case, it was of best interest to the experiment that both aerogel samples were of similar properties. Therefore, samples from the same batch, and of similar density were chosen, since the density of the material should have an effect on thermal conductivity (Berkeley National Laboratory, 2004). The position in the mold where the aerogels were located, with respect to placement of the hot press during fabrication, was also noted and recorded for each test in case this information proved to be necessary later in the experiment.

After the appropriate samples were selected, placed in the holder with the sensor and secured, the test procedure could begin. The Keithly Bridge standard experiment was utilized with 0.009 watts of power supplied to the C5465, Kapton disk (size indicated previously) for 12 seconds of measuring time for a single measurement.

Once the measurement was balanced and the initial data recorded the calculations could be completed. For this investigation, a fine tuned analysis was performed and time correction was used to compensate for the time delay of the computer with respect to the

recorded values. From the analysis, thermal conductivity, thermal diffusivity and specific heat were recorded.

3.5 Transmittance Measurements

Before any transmittance measurements could be obtained, it was necessary to design a device to hold the aerogels in the path of the light beam. This is because the aerogel samples fabricated were too big to fit in a standard cuvette and it was preferred that they not be destroyed for the experiment. The requirements of the design were that the aerogels maintain monolithic form for the experiment, that the beam enter and exit the sample through a flat (not curved) plane, and that the samples were easily placed in and removed from the instrument.

The base of the attachment, including screw holes for support, was pre-fashioned by another student and used as the starting point for the aerogel holder design. The original idea was to have a v-shaped holder that contacted only two points along the circular cross section of the aerogel to hold it up to the height of the beam. However, it was found that the beam was very low to the base used for the attachment, so the design was slightly modified so that the aerogel would sit lower on the base. The final attachment piece was designed in SolidWorks and then printed using the mechanical engineering department's 3-D printer. (See Appendix D: SolidWorks Aerogel Sample Holder for Reflectometer.)

The Perkin Elmer Lambda 900 UV/VIS/NIR Spectrometer was used to take transmittance measurements. Before each set of measurements were taken, baseline scans were taken of air. Then, percent transmittance was measured across the entire spectrum, ranging from 200-3000 nanometers, for each aerogel sample referenced to air and

recorded in separate files. (See Appendix F: Reflectometer Set-Up and Measurement Procedure.)

3.6 Fluorescence Measurements

A Photon Technology International Fluorometer system was used to take fluorescence measurements of the PtOEP-doped aerogel samples. The system utilizes an A-1010 Arc Lamp Housing, a model 814 Photomultiplier Detection System and a model LPS-220B Lamp Power Supply. (See Appendix G: Fluorometer Set-Up and Measurement Procedure.)

Samples were first prepared for the analysis. Using a knife, the aerogel samples were cut into pieces small enough to insert into a standard 10 x 10 x 45 mm polystyrene cuvette, trying as best as possible to keep the pieces monolithic and without jagged edges. The cuvette caps were labeled with the amount of water used to fabricate the sample and the piece number. Then, the sample cuvettes were wiped down with a Kimwipe to clean off any finger prints and inserted into the holder in the fluorometer (Plata, 2003). The labeled caps, however, were removed during the measurements and replaced with the cap attached to the gas proportioner system (Plata, 2003).

A 100% nitrogen environment was created using a nitrogen tank. Through the use of a series of connecting tubes, the nitrogen flow was directed from the tank to a gas proportioner, and then to a custom made cuvette cap, kept in the fluorometer. The cap has one tube that directs the flow into the cuvette to the sample, and another tube that directs the flow of nitrogen out into the surroundings as a vent.

3.6.1 Emission Scans

For an emission scan, the first acquisition file labeled "ovalene" was used. The aerogel samples, doped with PtOEP, were excited at a wavelength of 533 nanometers. Emission was expected to occur at 646 nanometers (Briones, 2003); therefore, the emission range was set to 610-710 nanometers (nm). Emission and excitation slits were both set to 2 nm. Emission scans were performed on each aerogel sample both in an air environment and under a 100% nitrogen flow.

3.6.2 Time-Based Scans

For a time-based scan the file labeled "O2 rate" was selected. The aerogel samples, doped with PtOEP, were excited at a wavelength of 533 nanometers. Emission was expected to occur at 646 nanometers (Briones, 2003); therefore, the detector was set to this wavelength. Data points of fluorescence intensity were taken at 0.5 points per second for up to 2400 seconds of data. Emission and excitation slits were both set to 2 nm. For each aerogel sample, the emission spectrum was taken under ambient conditions for 1-4 minutes until the signal stabilized. Then, using the gas proportioner, the flow of nitrogen was increased from 0 milliliters/minute (mL/min) to *approximately* 2000 mL/min and kept at this rate until the higher signal stabilized. The flow of nitrogen was turned off so that the signal decreased and stabilized again. Once the nitrogen flow was turned on again and the signal was stable, the time-based acquisition was stopped.

4 Data Analysis and Results

The chemical precursor "recipe" was altered by decreasing and increasing the amount of water used by a percent of the "standard" volume, which was 5.40 mL (see recipe in Appendix A). The density, thermal conductivity, percent transmittance and fluorescence intensity of each aerogel were then measured and compared to those of aerogels made using the standard, unaltered, recipe. The following table indicates the amount of water used for each batch investigated and Figure 4 shows a graphical representation of this information.

Table 1: Amount of Water Used for Aerogel Recipes

Batch	Amount of Water Used	Molar Ratio H_2O /TMOS
50% Decrease	2.70 mL	1.74
40% Decrease	3.24 mL	2.09
30% Decrease	3.78 mL	2.44
25% Decrease	4.05 mL	2.61
20% Decrease	4.32 mL	2.78
10% Decrease	4.86 mL	3.13
Standard Recipe	5.40 mL	3.48
10% Increase	5.94 mL	3.83
20% Increase	5.94 mL	4.18
25% Increase	6.48 mL	4.35
30% Increase	6.75 mL	4.52
40% Increase	7.02 mL	4.87
50% Increase	7.56 mL	5.22

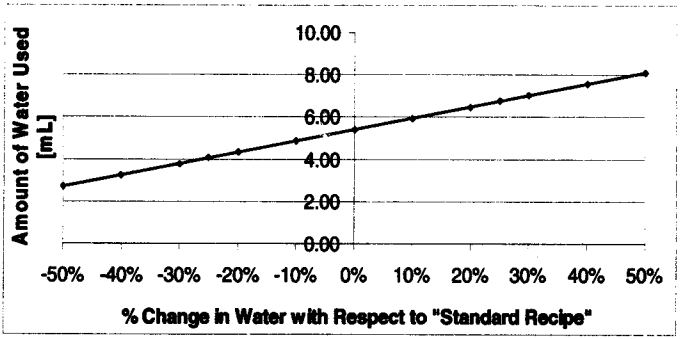

Figure 4: Amount of Water Used for Aerogel Recipes

4.1 Density

When calculating the density of an aerogel sample, there were uncertainties in the measurements used in the calculation that had to be taken into consideration. Most simply there was the uncertainty of the caliper used to measure the length and diameter of each aerogel sample: $\pm$0.0005 inches, half the size of the smallest available tick mark on the tool. A more significant uncertainty was due to the location where the measurement of the diameter of the sample was taken. Some aerogels shrank slightly when they were fabricated, which caused them to deviate from the cylindrical shape assumed for the calculation and form more of a "bowed" structure (see Figure 5). This created a discrepancy among the diameter values taken at the top, middle or bottom of the same sample. It was also noticed that another significant uncertainty was simply

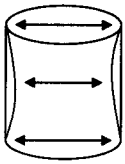

Figure 5: Bowed Structure as a Result of Aerogel Shrinkage

due to the ability to measure this type of material with a caliper accurately. The caliper is a sharp measuring tool that clamps the aerogel when used to measure the sample. Since the aerogel samples were very fragile they were easily squeezed slightly and deformed by the prongs of the caliper when they were measured, which would decrease the measured value of height or diameter from its true value. In an attempt to make the measurement slightly more repeatable, the condition was set that the value of height or diameter would be recorded when the caliper closed just enough for the sample to be held within the prongs without falling. However, it was still necessary to assess the repeatability of these recorded values.

To evaluate the two uncertainties, the diameters at the top, middle and bottom of a sample were each measured three times for 45 different aerogel monoliths and the values recorded. From this information, the standard deviation of the values recorded for the diameter measured at the top, middle, and bottom of the same aerogel were used to assess the uncertainty in the cylindrical shape of the samples. Similarly, the standard deviation of the values recorded each time the diameter was measured in the same place (top, middle or bottom) on the same aerogel was calculated to assess the repeatability of the measurements. The procedure was repeated for 45 different aerogel samples so that the standard deviation values could be averaged to find an overall uncertainty: one for the cylindrical shape of the aerogels and one for the repeatability of a measurements using the caliper. The uncertainty of the *diameter* from the top of an aerogel sample to the bottom was found to be $\pm$ 0.006 inches, and the uncertainty of the measurement made on an aerogel with the caliper, which can be applied to both the diameter *and* the height measurements was found to be approximately the same at $\pm$ 0.007 inches.

For the measurement of diameter these three types of uncertainties discussed were considered additive, making the total uncertainty for this measurement $\pm$ 0.014 inches. For height, however, the uncertainty in the cylindrical shape does not apply and therefore, the total uncertainty for this measurement was $\pm$ 0.0075 inches. Using the average length and diameter of the 45 aerogel samples used, which were 0.658 inches and 0.845 inches, respectively, an estimate of uncertainty in volume was calculated according to the equation: Volume = $(H\pi D^2)/4$.

$$\text{Uncertainty in Volume} = \sqrt{\left(\frac{0.0075}{0.658}\right)^2 + \left(\frac{0.014}{0.845}\right)^2 + \left(\frac{0.014}{0.845}\right)^2} = 0.02_5 \text{ in}^3 = 0.06_4 \text{ cm}^3$$

The uncertainty in the mass measurement was assumed to be the lowest decimal reported by the balance used, it was $\pm$ 0.0001 grams. Taking into consideration the average mass and volume of the aerogel samples, 0.5517 grams and 6.02_1 cm^3, respectively, and the equation used to calculate density: D = M/V, the uncertainty in the density values was calculated.

$$\text{Uncertainty in Density} = \sqrt{\left(\frac{0.06_4}{6.02_1}\right)^2 + \left(\frac{0.0001}{0.5517}\right)^2} = 0.01_1 \text{ g/cm}^3$$

The investigation has found that increasing and decreasing the amount of water used in the pre-fabrication chemical recipe does not significantly alter the density of the aerogel monoliths produced within the range of -50%/+50% of the water content in the standard aerogel recipe by volume. To see if there were any observable trends, the densities of the aerogels from each altered batch were plotted on a graph displaying density as a function of sample position with respect to the hot press shown in Figure 4 below. (Key for Figure 6 can be found in Table 2.)

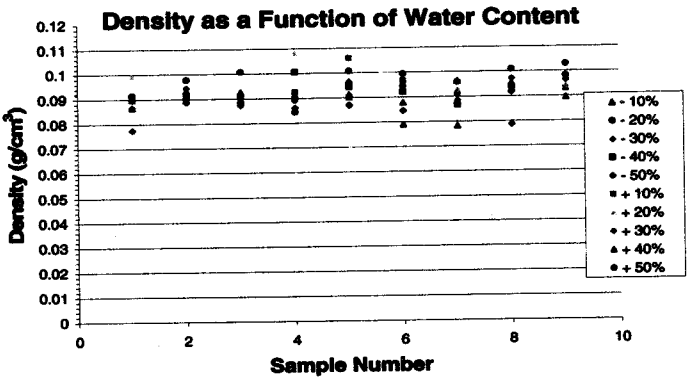

Figure 6: Density as a Function of Water Content with Respect to Sample Position

1	2	3
4	5	6
7	8	9

(Front of Hotpress)

Figure 7: Sample Position in Hotpress

The average density of the aerogels for each altered batch were then calculated and compared to the average density of standard aerogels made using the "standard" recipe.

Table 2: Average Density for Aerogels with Increased/Decreased Water Content

Batch	Average Density [g/cm^3]
[redacted]	0.09_6
[redacted]	0.08_9
[redacted]	0.09_1
[redacted]	0.09_4
[redacted]	0.09_4
Standard	0.09_1
[redacted]	0.09_5
[redacted]	0.09_5
[redacted]	0.09_2
[redacted]	0.09_2
[redacted]	0.08_6

Figure 6, and Table 2 more specifically, show that the densities of all of the aerogels are approximately 0.09 g/cm^3. Within the uncertainty calculated, $\pm$ 0.01 g/cm^3, the average densities of each of the aerogel batches are not significantly different from the other batches. Therefore, we have concluded that the amount of water in the precursor mixture did not affect the density of these aerogels.

4.2 Thermal Conductivity

We have shown that increasing and decreasing the amount of water used in the pre-fabrication chemical recipe did not significantly alter the thermal conductivity of the aerogel monoliths that were produced using as much as 50% more water (by volume) than the standard recipe and as little as 50% less water (by volume) than the standard recipe. The average thermal conductivity for each altered batch was calculated and compared to that of the aerogels made using the standard recipe to see if there were any observable trends. The uncertainty of the thermal analyzer was unknown, therefore the

thermal conductivity values reported in Table 3 were only shown to one significant figure for evaluation.

Table 3: Average Thermal Conductivity for Aerogels with Increased/Decreased Water Content

Batch	Thermal Conductivity [W/mK]
50% Increase	0.04_3
40% Increase	0.03_9
30% Increase	0.04_2
20% Increase	0.04_3
10% Increase	0.04_1
Standards	0.04_2
10% Decrease	0.04_1
20% Decrease	0.04_2
30% Decrease	0.04_1
40% Decrease	0.04_2
50% Decrease	0.04_2

Table 3 shows that there was no significant change in the thermal conductivity of the aerogels as the amount of water used in the chemical recipe is increased or decreased. The values of thermal conductivity are approximately 0.04 W/mK for all of the aerogels fabricated in this experiment.

4.3 Transmittance

While in the process of measuring density and thermal conductivity for aerogels of increased and decreased water content, it was noticed that there was an observable trend in the amount of light that was able to pass through the samples, also known as the transmittance of the aerogel. Even to the naked eye it was apparent that there was an

increase in the amount of visible light that passed through the aerogel samples as the amount of water used was increased. The aerogels became cloudier and opaque as the water content used was decreased. An aerogel made with 50% decreased water content by volume appeared opaque and dark when it was held up to the light (see Figure 8); however, an aerogel made with 30% increase in water was much more transparent. Note that the dark spot on the back of the beaker could be seen through the aerogel when it was held up to a regular lamp (room light). (See Figure 8.)

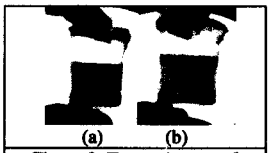

Figure 8: Transmittance of Room Light through Aerogels of a) 50% Decrease in Water, b) 30% Increase in Water

In order to obtain precise transmittance measurements, a reflectometer was employed. To assess the uncertainty of the measurement, each sample was measured twice. Figure 9 shows the spectrum of the first run for each aerogel sample.

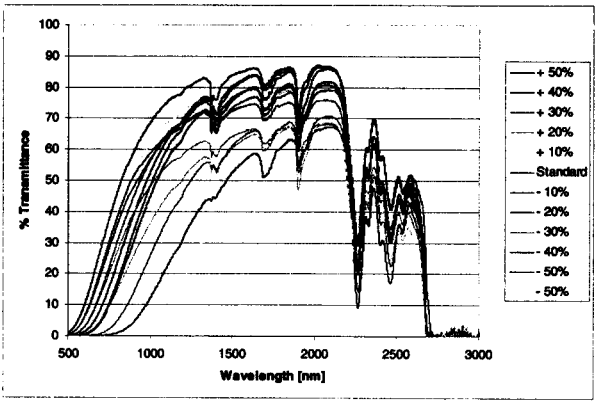

Figure 9: Percent Transmittance of Aerogel Samples at each Wavelength in the Range of 500-300 nm (Referenced to an Air Blank)

The peaks in the near infrared region of this spectrum at 1400, 1700, 1900, 2250 and 2500 nm are characteristic of aerogel samples (Berkley National Laboratory, 2004). They correspond to an absorbance of light due to the chemical composition of the aerogels. In the visible region of the spectrum the percent of light that is transmitted through the sample decreases as the wavelength gets smaller for all of the samples. It is also in this region that the spectrum of each sample seems to diverge from one another most. This is expected since scattering prevents light from transmitting and this effect intensifies as the wavelength of light decreases ($I_{scatter} \propto 1/\lambda^4$). For this reason, it was this area that was focused on when comparing the aerogel samples made with increased and decreased amounts of water to one another and the standard recipe. Figures 10 and 11 both show a closer look at this region of the spectrum for the first and second run of the aerogel samples. The only difference between these two runs was the repositioning of the sample.

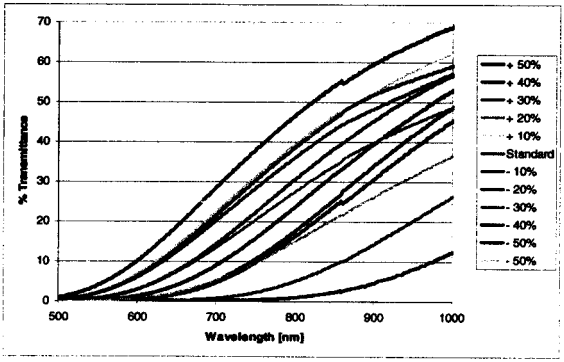

Figure 10: Transmittance of Aerogel Samples in the Range from 500-1000 nm (Run #1) (Referenced to an Air Blank)

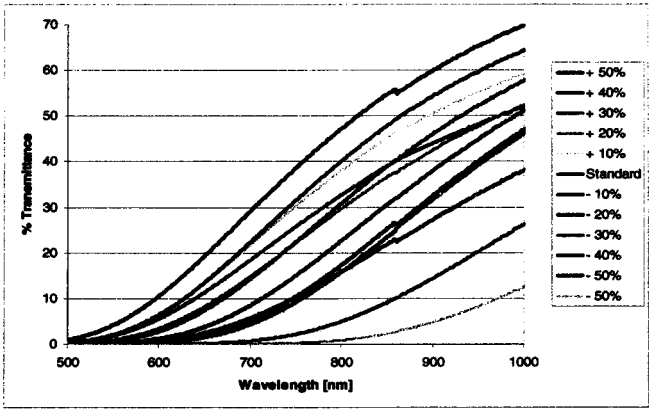

Figure 11: Transmittance of Aerogel Samples in the Range from 500-1000 nm (Run #2) (Reference to an Air Blank)

Comparing Run #1 to Run #2 shows that there is a slight variation in transmittance each time a measurement is taken. Some samples displayed an overall increase in transmittance throughout the visible region, some showed an overall decrease, and others only diverged in certain parts of the region plotted. This uncertainty should be taken into consideration when analyzing the data.

In both Figure 10 and 11, one can see that the trend that was expected based solely on visual observation was in fact illustrated in these results. As the amount of water used to fabricate the aerogels is decreased, the percent transmittance through the sample also decreases. The sample with a 50% increase in water (with respect to the "standard" recipe) had the most light transmitted through it in this region and the sample

with 50% decrease in water (with respect to the "standard" recipe) had the least amount of light transmitted through it in this region. Although the overall trend seems to follow the expected hypothesis, the data does not adhere to the trend exactly. One can see that the data from a standard aerogel sample, though expected to be toward the middle of the group, seems to be transmitting more light than expected. Similarly, the sample with a 10% decrease in water content seems to be transmitting more light than the sample with a 40% increase in water. (See Figure 10 and 11) Though some of these discrepancies can be attributed to the uncertainty of the instrument, further investigation was sought.

It was at this point in the investigation that other members of the group had been experiencing difficulty making suitably transparent aerogels. In order to fix this problem, new solutions were made and collected to replace the old, possibly contaminated bottles. In the midst of this process, it was discovered that the solution of base catalyst was the problem, having possibly absorbed carbon dioxide from the air. Aqueous solutions pick up this weak acid from the atmosphere becoming more dilute with the loss of NH_3 ($H_2O_{(l)} + NH_{3(aq)} + CO_{2(g)} \rightarrow HCO_3^- + NH_4^+$) and, hence, slow the gelation process. Upon its replacement with a fresh solution of 1.5 M NH_4OH, aerogel samples that were even more transparent then the previous best were fabricated. This may have caused the transmittance results taken for the aerogels fabricated before this problem was discovered to be unreliable (those shown in Figures 10 and 11), considering the very *noticeable* effect the concentration of the catalyst had on the transparency of the aerogels. Therefore, new aerogel samples were fabricated within the same range (-50%/+50% of the water content in the standard aerogel recipe by volume) using the replaced chemicals and transmittance measurements were repeated. The results can be found in Figure 12 below.

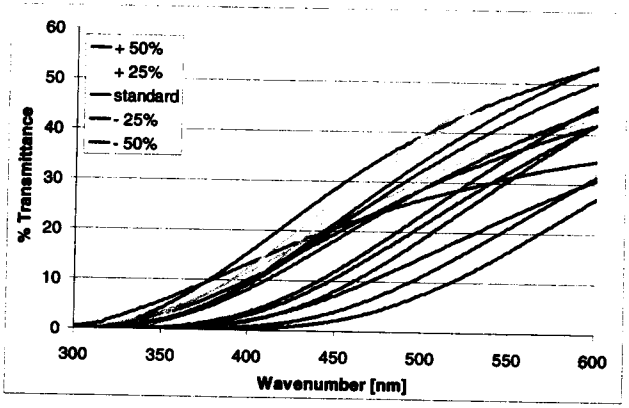

Figure 12: Percent Transmittance of Aerogel Samples in the Range 300-600 nm (Reference to an Air Blank)

By comparing the data in Figure 12 to that in Figures 10 or 11 at 500 nm, it can be seen that the percent transmittance of these new aerogels had increased greatly. For example, in Figures 10 or 11, average signal is approximately 5% transmittance, while in Figure 12, at the same wavelength, the average signal at 600 nanometers is approximately 45% transmittance.

Though there was a significant increase in the transparency of the aerogel as a result of the new catalyst, the trend that more water produces a more transparent aerogel remained. Figure 12 also shows that, as the amount of water used to fabricate the aerogels decreased, the percent transmittance through the samples decreased as well. There are a few discrepancies, particularly with the 50% increased water aerogel samples, where the variation among those samples seems to be higher than the rest of the samples. However,

these were the first measurements taken and may have been due to the instrument having been not completely warmed up.

4.4 Fluorescence of PtOEP-Doped Aerogels

4.4.1.1 Emission Scans

Emission scans of PtOEP-doped aerogels were taken in both a 100% nitrogen environment and an air environment in which the fluorescence of PtOEP is quenched by the presence of approximately 21.5% oxygen. The fluorescence emission spectrum in Figure 13 shows that aerogels have been doped successfully with PtOEP. When the PtOEP-doped aerogels were in ambient conditions the emission spectra showed no fluorescence peak at 646 nm. However, it is known that the fluorescence of this chemical is quenched in the presence of oxygen and air contains approximately 21.5% oxygen. Therefore, a 100% nitrogen environment was applied to the aerogel. In these conditions (i.e. in the absence of oxygen), the aerogels display fluorescence. The fluorescence intensity of each PtOEP-doped aerogel increased significantly in the nitrogen environment. Figure 13 shows this response for the aerogel sample made with 50% decreased amount of water with respect to the "standard" recipe.

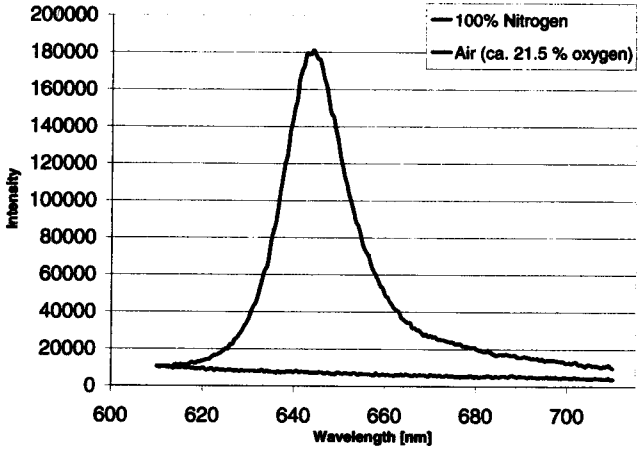

Figure 13: Fluorescence of PtOEP-Doped Aerogel Sample (50% Decrease in Water)

Although each doped aerogel sample showed a similar response, the extent to which the fluorescence intensity increased was different (see Appendix H: Emission Spectra of PtOEP Doped Aerogels in 100% Nitrogen.) However, because each doped aerogel sample was fabricated with a slightly different concentration of PtOEP (due to variation in total volume of the precursor mixture), the intensity of the sample in the nitrogen environment could not be compared directly. Instead, the ratio of average fluorescence intensity in 100% nitrogen (0% oxygen), $F_{100\% N2}$, to that in the presence of air (ca. 21.5% oxygen), F_{air}, was compared. Table 4 shows that this ratio is not constant for all the aerogels. (See Appendix I: $F_{(100\% N2)}/F_{(Air)}$ for Each PtOEP Doped Aerogel.)

Table 4: Average Fluorescence Intensity Ratio for PtOEP-Doped Aerogel Samples

Aerogel Sample	$\frac{F_{(100\% Nitrogen)}}{F_{(Air)}}$
50% Increase	2.4
25% Increase	5.4
Standard	3.7
25% Decrease	5.1
30% Decrease	30
40% Decrease	67
50% Decrease	22

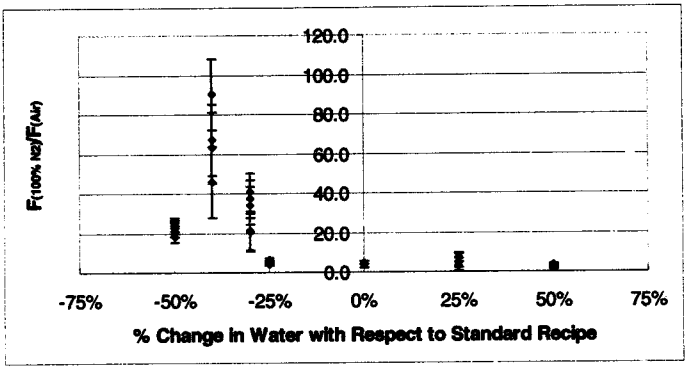

Figure 14: Graphical Representation Comparing Fluorescence Intensity Ratio for PtOEP-Doped Aerogel Samples

The data shows that the amount of water used to make the aerogels affects the response an aerogel will produce as an oxygen sensor utilizing PtOEP. The PtOEP-doped aerogels made with a 40% decrease in water have significantly greater response than any of the other samples.

4.4.1.2 Time-Based Scans

Time-based scans of the PtOEP-doped aerogels were taken to demonstrate whether the aerogels would display a reversible response and how quickly they would detect the presence of oxygen. The time-based scan in Figure 15 shows that we have, indeed, created a reversible sensor with a fast response.

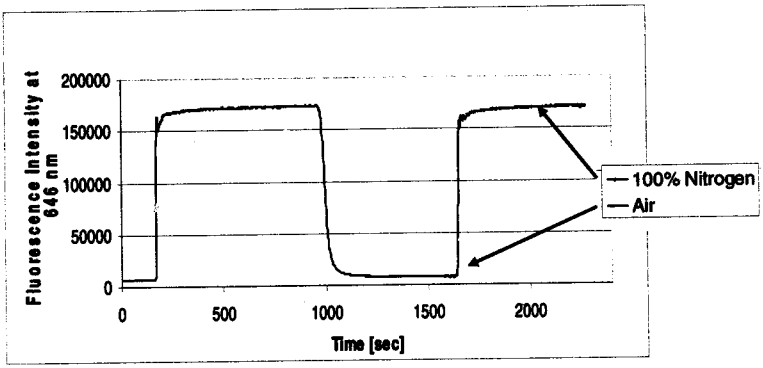

Figure 15: Fluorescence Intensity at 646 nm as a Function of Time for PtOEP-Doped Aerogel Sample Made with 50% Decreased Water (λ_{ex}=533 nm)

When oxygen is present (in the air), the fluorescence of the doped aerogel sample was quenched; as the sample was introduced to a 100% nitrogen environment, the intensity increased and stabilized. The nitrogen flow was then shut off (after approximately 12 minutes for the data in Figure 15, however this time varies depending on the run), and as a result of the incoming air, the fluorescence signal decreased as it was quenched by the oxygen present. The process was then repeated and produced the

same results showing that it is reversible. During the experiment, the fluorescence intensity increased as the knob controlling the flow of nitrogen was turned; this shows that the doped aerogel samples display a real time response that may have even been faster if the flow could be applied more quickly. (See Appendix J: Time based Spectra of PtOEP-Doped Aerogels.)

5 Discussion of Results

5.1 Density

The results from this investigation are that the density of the fabricated aerogels was not affected by the amount of water used in the precursor solution. However, these were not the expected results based on the literature (Rao et al., 1994). In this investigation, the mole ratio of the amount of water to TMOS used ranged from approximately 2 to 5. Within this range, it was expected, from the work of Rao et al. that the change in density should decrease significantly as the molar ratio of H_2O:TMOS is increased. Figure 16 shows a direct comparison between the results obtained by Rao et al. and the results obtained in this investigation.

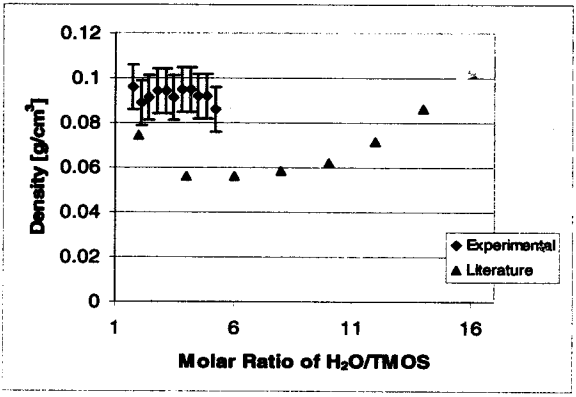

Figure 16: Experimental and Literature Comparison of Density as a Function of Molar Ratio of H_2O/TMOS (Rao et al., 1994)

In Figure 16, it is clearly shown that the experimental results deviate from the literature trend. The experimental aerogel samples fabricated are, on average, denser than the ones found by Rao et al. In addition, we do not see the same decrease in density as the molar ratio of water to TMOS increases from 2 to 4; the experimental results, instead, does not vary significantly from 0.09 g/cm^3.

An explanation for this difference in trend from what was expected could be due to the difference in the precursors used to make aerogels. Our recipe uses slightly smaller molar ratios of methanol to TMOS and of TMOS to NH_4OH. The experimental molar ratios were 11.88 and 3.5×10^{-3} (respectively) whereas the literature values were 12 and 3.7×10^{-3} (respectively).

The fact that the densities of our aerogel samples do not significantly change as the amount of water is changed may also be due to a significant difference in the fabrication process. In the literature, pH was measured and carefully indicated, the solution was allowed to gel before the supercritical extraction process was carried out, an autoclave was used with a nitrogen gas flush, and the final aerogel was heated in air at the end of the process (Rao et al., 1994). In the Union Rapid Supercritical Extraction process, however, the solution is mixed for a few minutes, pH is not observed, and the solution is then left in the hot press to gel and reach supercritical state before extraction, all under the temperature and pressure program of the machine.

The fast supercritical extraction method invented at Union already has an advantage over the conventional method because it is a one-step process that takes much less time. In addition, what this experiment may have shown is that another advantage may be that the resulting aerogels are more uniform in some physical properties,

including density. However, this could also be considered a disadvantage when the desire is to better control the physical property of this material for a specific purpose.

5.2 Thermal Conductivity

The thermal conductivity results are that as the amount of water used in the precursor recipe increases or decreases, the insulating properties of the resulting aerogels do not change significantly (see Table 3 in the results section). The average thermal conductivity for our aerogel samples was approximately 0.04 W/mK. This value is higher than the literature values stated by Berkeley National Laboratory, which range from as low as 0.008 W/mK to 0.017 W/mK.

The reason aerogels are so thermally insulating has to do with the way heat travels through this material. Heat transfer can occur in three ways in an aerogel: it can be conducted through solid, it can be conducted through gas, and it can be transferred by means of radiation. Convection also exists in this case; however, it is not separate from gas conduction because there is no "mean flow" by either natural or forced convection. In aerogels, the structure is made of only 1-10% solid silica spheroids and the matrix is composed of a chain-like structure that has many branches and "dead ends" to the solid material (Berkley National Laboratory, 2004). As heat travels through the solid portion of the aerogel, it can branch off and hit a "dead end" where the solid matrix hits a pore, which will stop the conduction of heat through this solid. Similarly, if heat is conducting through air inside one of these pores, it can also come to a stop if it hits the solid pore wall. Gas conduction occurs when one gas molecule hits another. But in the aerogel matrix the mean free path (the distance a molecule travels before hitting another) is approximately the same size a as pore; therefore, it is more likely that the gas molecule

will hit the solid wall before another gas molecule. The intricate weaving of pores and solid branches in the matrix makes it difficult for heat to find a continual path through the material. The third method of heat transfer, radiation, only takes places at very high temperatures; therefore, it does not significantly facilitate the transfer of heat throughout an aerogel in the conditions of this study. It is for these reasons that aerogels are so uniquely insulating.

Thermal conductivity of aerogels is affected mostly by the amount of solid, the structure of the matrix and the size or distribution of the pores. If there is more solid and the matrix has fewer "dead ends," then the thermal conductivity should increase as the transport of heat through solid conduction increases. Similarly, if the material has larger pores, then more air is entrapped, allowing gaseous conduction to facilitate the transfer of heat and increase the thermal conductivity. This indicates that density should be related to thermal conductivity. The density of an aerogel indicates how much solid silica is present in a certain volume of the material. The denser an aerogel, the more silica is present and as a result the smaller the pores must be. Because we have seen that the density of the aerogels does not change significantly as the molar ratio of TMOS to H_2O is varied, it is reasonable that the thermal conductivity does not vary as well. The amount of silica or size of the pores might not be altered enough to affect the thermal conductivity. Berkley National Laboratory does not indicate the density of the aerogels used in their thermal conductivity tests. Therefore, a difference in density could be the reason our aerogels have higher thermal conductivities.

5.3 Transmittance

The results of this investigation are that the average percent transmittance of an aerogel (in the visible region) decreases as the amount of water used in the precursor solution is decreased. Rao et al. focused on transmission at 900 nm. Based on their work, as the molar ratio of water to TMOS increases from approximately 2 to 5, the percent transmission through the aerogel samples should increase and then plateau at approximately 90% transmittance (see Figure 17 below). However, the experimental data from this investigation is not consistent with the literature results. As the molar ratio of water to TMOS is increased from 2 to 4, the percent transmission is level at first around approximately 70% and then, after further increase in the ratio to 5, it starts to decrease very slightly (see Figure 17). The error bars in Figure 17 represent the standard deviation of transmittance at 900 nm for each aerogel sample made with the same molar ratio of water to TMOS.

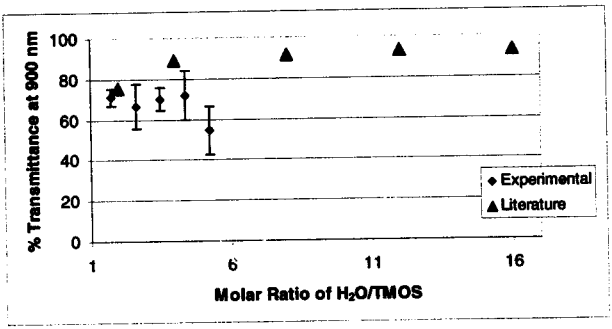

Figure 17: Experimental and Literature Comparison of Transmittance at 900 nm as a Function of Molar Ratio of H_2O/TMOS (Rao et al., 1994)

This particular wavelength (900 nm) was not the focus of the experimental investigation because this investigation is for the purpose of developing aerogel platform optical sensors, which are required to be transparent in the visible region in order to take proper fluorescent measurements. In our experiment the transmittance measurements at 900 nm did not show the same trend that was found in the near the visible region. There was also more variation in the results between samples made with the same amount of water; this variation is illustrated in Figure 18.

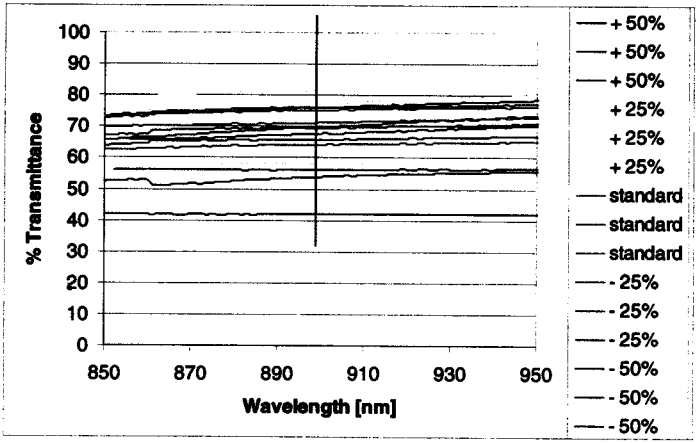

Figure 18: Variation in Percent Transmittance of Aerogel Samples at 900 nm

Further focus in this region is necessary, to decrease the amount of variation in order to better analyze the trend associated with these results. However, we can note without

looking at the trend that our values are on the same order of magnitude as Rao et al.'s results, approximately 70%.

Without comparing to the literature we can still draw some conclusions from our results. Transmittance is a measure of how much light traverses through a sample. The more light is scattered by the aerogel, the less it transmits. Therefore, a variation in the amount of light transmitted through an aerogel may be an indication that the light is scattering in different ways. Rao et al. noted that the amount of water used to make aerogels will determine the "distribution and number" of monomers resulting from the hydrolysis reaction and available for condensation. Therefore, it should have a significant effect on the formation of the silica matrix. The amount of water used in the precursor solution could be affecting the pore size of the resulting aerogel and the pattern or structure of the matrix, altering the path of light through the material.

5.4 Fluorescence Study

The fact that the aerogels show a quantifiable fluorescence signal in the absence of oxygen (in a 100% nitrogen environment) shows that the fluorescent probe, PtOEP survived the high temperatures and pressures of the Union Rapid Supercritical Extraction aerogel fabrication process without decomposing (see Figure 13). In addition, the aerogels in ambient conditions (Air: 21.5% oxygen) do not show a significant fluorescence signal, indicating that most, if not all, of the entrapped probe, is accessible to oxygen within the aerogel matrix.

The time-based scans show that the response time of the aerogel when exposed to the 100% nitrogen flow is on the order of 10 seconds. When the flow of nitrogen is then turned off and air is allowed to diffuse into the environment, the aerogel's response to

this change is slightly longer, ranging from 30-60 seconds (see Figure 14). This may be longer as a result of the slow rate at which the gas can diffuse into the instrument's sample compartment or it may be because oxygen diffuses into the aerogel matrix slower than nitrogen does, as was found in Lee and Okura's work (1997).

We wanted to prepare Stern-Volmer plots to assess the relationship between fluorescence intensity and quencher concentration. However, it was found that the fluorescence of the PtOEP-doped aerogels was being quenched by such small percentages of oxygen (on the order of 1%) that the sensor response was ultimately acting like a switch. The gas proportioner could not restrict the flow of air and nitrogen under approximately 1000 mL/min with accurate measurements, therefore it was not sensitive enough to create the appropriate gas mixtures necessary to perform the experiment. The fact that the aerogels were so sensitive to oxygen indicates that the probe inside the aerogel matrix must be extremely accessible to this gas.

When the amount of water used in the precursor solution was altered, the sensitivity of the PtOEP-doped aerogels to oxygen changed. The ratio of fluorescence intensity in 100% Nitrogen to that in air (21.5% oxygen) ranged from approximately 2 to 20 (see Table 4 in the results section). The values at the lower end of this range made with 6.48 mL (a 25% decrease in water) water or more are slightly higher than Lee and Okura's literature values (1997). They found that sol-gels doped with PtOEP displayed a ratio of fluorescence intensity in 100% Nitrogen to that in approximately 21.5% oxygen ranging from approximately 0.5 and 2. The reason the literature values are slightly smaller may be because the probe is slightly less accessible to the gas since it is in a different environment.

An interesting change in the ratio of fluorescence intensity in 100% nitrogen to that in air occurred specifically when the water was *decreased* from 6.48 mL (25% decrease) to 6.75 mL (30% decrease); the aerogels experienced a significant *increase* in this ratio from 5.1 to 31 (see Table 4 in the results section). This indicates that the PtOEP probes are more accessible in the aerogels made with less water than those made with more. Like the other physical properties that were investigated, this could be a result of a difference in the formation of the matrix that affects its pattern and the size of its pores. This could affect the probe's accessibility to oxygen within the matrix or the rate at which oxygen can diffuse into the material.

6 Conclusions and Future Work

This investigation has shown that the amount of water used in the fabrication of silica aerogels does, in fact, have an effect on some of the physical properties of the resulting samples. We have found that the densities and thermal conductivities of the aerogels were not significantly altered as the amount of water was changed. All the aerogels produced in this investigation displayed densities of approximately 0.09 g/cm^3 and thermal conductivities of 0.09 W/mK. However, the transparency of each aerogel *was* affected by this modification. Using more water in the precursor solution made the resulting aerogels more transparent.

Because transparency is an advantage for optical sensors utilizing fluorescent probes, the study was extended to investigate aerogels doped with an oxygen sensing complex, PtOEP. This luminescent probe was successfully entrapped inside the matrix of several aerogel samples using Union's Fast Supercritical Extraction method. The results of spectral characterization show that PtOEP-doped aerogels will produce a better response to oxygen, a higher ratio of fluorescence intensity in 100% nitrogen to that in air (21.5% oxygen), if the amount of water used in the fabrication process is *decreased.*

There are some limitations to this investigation, however, that could possibly be resolved through future work. First, the range in which the amount of water was increased or decreased was limited to $\pm$ 50% the volume of water in the standard recipe (see Appendix A). This range could be extended to investigate the physical properties of silica aerogels made with higher or lower amounts of water.

Another area that demands further investigation is the cause of the change in transparency of the aerogels. The amount of light that transmits through an aerogel is a

result of the way light scatters as it passes through the sample. We hypothesize that light is scattered depending on the size and distribution of pores in the aerogel; therefore, an increase or decrease in the amount of water used to fabricate the samples might be affecting the structure of the matrix. To help verify this theory, it would be useful to have data on pore sizes and distribution using the gas adsorption system for aerogels made with different amounts of water. This may provide insight as to why the density and thermal conductivity of the aerogels do not seem to change significantly, while the aerogels become more transparent as the amount of water used in the precursor mixture is increased.

In the fluorescence study it was found that there was a significant increase in the ratio of fluorescence intensity in 100% nitrogen to that in air (21.5% oxygen) when the amount of water was decreased from 6.48 mL (25% decrease) to 6.75 mL (30% decrease). It is also evident from the results that the most sensitive aerogel samples, the ones with the highest ratio of fluorescence intensity in 100% nitrogen to that in air (21.5% oxygen), were made with 7.02 mL (40% decrease) of water. More data is needed to explain why there is such a significant increase in sensitivity with only a small decrease in water, and why a 40% decrease in water from the standard recipe produced the best response to oxygen for the PtOEP-doped aerogels. It would be useful to test the repeatability of these results because the $F_{(100\% N2)}/F_{(air)}$ ratio varied significantly between samples. Similarly, additional data points could be taken within the range of water used (i.e. altering the amount of water used with respect to the standard recipe at an interval of 2% rather than 5-10%).

Future work should also be done to extend the investigation of the PtOEP-doped aerogels to include fluorescence lifetime analysis. This information would be useful to characterize the microenvironments of the fluorescent probe. Lifetime data would provide evidence as to where the probe is located in the silicon-oxygen matrix and allow us to assess its accessibility to oxygen more completely. It might then be possible to relate this information to the change in sensitivity the PtOEP-doped aerogels display when the amount of water used to fabricate the samples is altered.

In this investigation an *attempt* was made to create Stern Volmer plots for the PtOEP-doped aerogels. However, it was found that the samples were too sensitive to oxygen for the gas proportioner to deliver a small enough flow of nitrogen and air. To resolve this problem in the future, a gas delivery system that is more sensitive could be built or a new set of aerogels doped with a smaller concentration of PtOEP could be investigated.

Lastly, the work with PtOEP-doped aerogels should be extended to include aerogels made with a mixture of TMOS *and* ormosils. Using different ormosils should alter the structure of the aerogel matrix. Therefore, doping the samples with PtOEP and continuing with similar fluorescence studies should also offer information as to how these silica-based precursors affect the resulting aerogels. It would be interesting to see how the microenvironments of the probe compare to aerogels made solely with TMOS. Of particular focus would be to see how the probe's accessibility to oxygen and changes when different ormosils are used.

Each experiment will help explain how the silicon-oxygen matrix and the physical properties of an aerogel are affected by the precursors used in the fabrication process.

7 References

Aerogel. (1999). Retrieved December 10, 2002, from California Institute of Technology, Stardust Technology website: http://stardust.jpl.nasa.gov/tech/aerogel.html

Amao, Y., Asai, K., Okura, I., Shinohara, H., Nishide, H. (2000). "Platinum porphyrin embedded in poly(1-trimethlysilyl-1-propyne) film as an optical sensor for trace analysis of oxygen," The Analyst, Vol. 125, pp. 1911-1914.

Bakrania, S. (2002). *The Effect of Water, Catalyst and Solvent Content on Silica-Aerogel Density, Conductivity and Porosity*. Retrieved December 10, 2002, from http://tardis.union.edu/me_dept/me_dept.html

Brinker, C.J., Scherer, G.W., Sol-Gel Science, Academic Press, New York, 1990.

Ernest Orlando Lawrence Berkley National Laboratory. (2004). *Thermal Properties of Silica Aerogels*. Retrieved May 15, 2004 from http://eande.lbl.gov/ECS/aerogels/satcond.htm.

Ernest Orlando Lawrence Berkley National Laboratory. (2004). *Optical Properties of Silica Aerogels*. Retrieved June 5, 2004 from http://eande.lbl.gov/ECS/aerogels/saoptic.htm.

Gauthier, B. (2001). *Enhanced Aerogel Fabrication*. Retrieved December 10, 2002, from http://scoter.union.edu/~andersoa/Gauthier/Untitled%20Document.htm

Gauthier, B., Bakrania, S., Anderson, A., Carroll, M., (2004), "A Simplified Technique for Fabricating Aerogels Using Fast Supercritical Extraction," Journal of Non-Crystalline Solids, Vol. 350, pp. 238-243.

Kistler, S.S. (1932) J. Phys. Chem., Vol. 63, p. 52.

Lee, S.K., Okura, I. (1997). "Optical Sensor for Oxygen Using a Porphyrin-doped Sol-Gel Glass," The Analyst, Vol. 122, pp. 81-84.

Leventis, N., Elder, I., Rolison, D. R., Anderson, M. L., Merzbacher, C. I. (1999). "Durable Modification of Silica Aerogel Monoliths with Fluorescent 2,7-Diazapyrenium Moieties. Sensing Oxygen near the Speed of Open-Air Diffusion," Chem. Mater., Vol. 11, pp. 2837-2845.

Lu, X., Winnik, M. (2001). "Luminescence Quenching in Polymer/Filler Nanocomposite Films Used in Oxygen Sensors," Chem. Mater., Vol. 13, pp. 3449-3463.

Pierre, A.C., Pajonk, G.M. (2002). "Chemistry of Aerogels and Their Application." Chemistry Review, Vol. 102, pp. 4243-4265.

Plata, D., *Sol-Gel-Platform Optical Sensors For Oxygen Gas: Sensor Development and Investigation of Probe Partitioning in Sol-Gel Matrices*, 2003. (Senior Thesis)

Plata, D., Briones, Y., Wolfe, B., Carroll, M., Bakrania, S., Mandel, S., Anderson, A. (2004). "Aerogel-platform optical sensors for oxygen gas," Journal of Non-Crystalline Solids, Vol. 350, pp. 326-335.

Poco, J.F., Coronado, P.R., Pekala, R.W., Hrubesh, L.W. (1996). "A Rapid Supercritical Extraction Process for the Production of Silica Aerogels," Materials Research Society Symposium, Vol. 431, p. 297.

Rao, A.V, Pajonk, G.M. and Parvathy, N.N (1994) "Effect of solvents and catalysts on monolithicity and physical properties of silica aerogels", Journal of Materials Science, Vol. 29, pp. 1807-1817.

Roa, A.V, Pajonk, G.M. and Parvathy, N.N (1994) "Influence of Molar Ratios of Precursor, Catalyst, Solvent and Water on Monolithicity and Physical Properties of TMOS Silica Aerogels", Journal of Sol-Gel Science and Technology, Vol. 3, pp. 204-217.

Wagh, P.B., Begag, R., Pajonk, G.M., Rao, A.V., Haranath, D. (1999). "Composition of some physical properties of silica aerogel monoliths synthesized by different precursors", Materials Chemistry and Physics, Vol. 57, pp. 214-218.

8 Appendices

8.1 Appendix A: "Standard" Recipe

Precursor	Volume
TMOS	12.75 mL
Methanol	41.25 mL
Deionized water	5.40 mL
1.5 M Ammonium Hydroxide (catalyst)	0.200 mL

8.2 Appendix B: Solidworks Mold

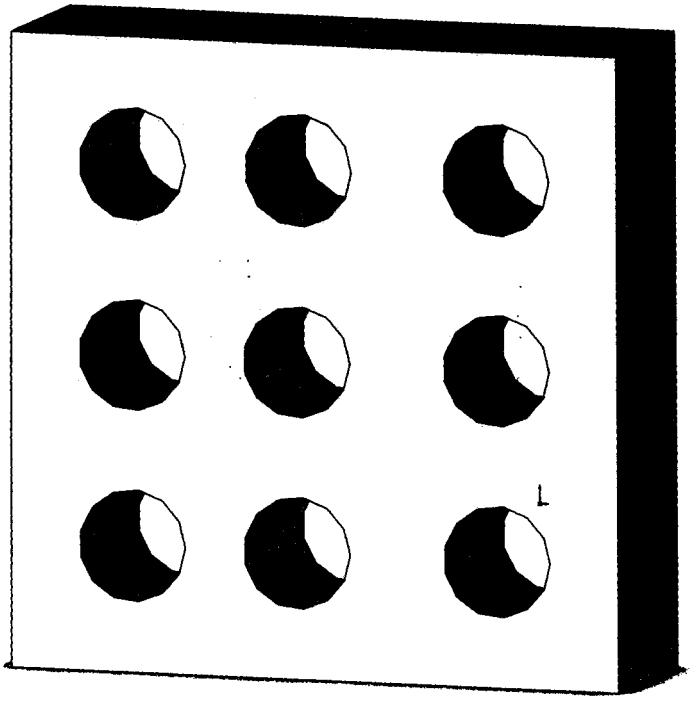

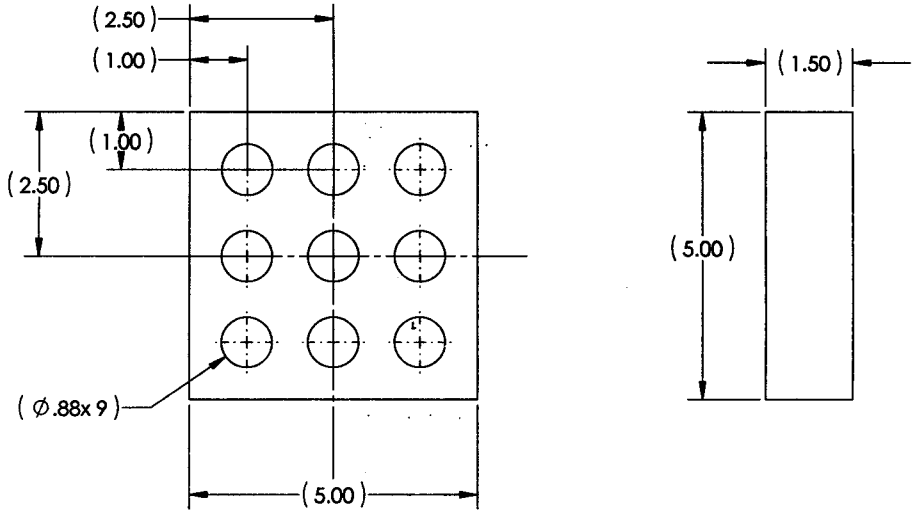

		UNLESS OTHERWISE SPECIFIED:		NAME	DATE
		DIMENSIONS ARE IN INCHES TOLERANCES: FRACTIONAL ± ANGULAR: MACH ± BEND ± TWO PLACE DECIMAL ± THREE PLACE DECIMAL ±	DRAWN		
			CHECKED		
			ENG APPR.		
			MFG APPR.		
		INTERPRET GEOMETRIC TOLERANCING PER:	Q.A.		
		MATERIAL	COMMENTS:		
NEXT ASSY	USED ON	FINISH			
APPLICATION		DO NOT SCALE DRAWING			

TITLE:

SIZE	DWG. NO.	REV
A	mold	
SCALE: 1:2	WEIGHT:	SHEET 1 OF 1

5 4 3 2 1

8.3 Appendix C: Hot Press Setup

Date:_____

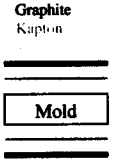

Hot press Program

	1	2	3	4	5	6
Temp. (°F)	100	550	550	550	550	100
Pressure (psi)	1040	1040	1040	150	150	150
Time (H:M:S)	0:2:0	3:0:0	0:30:0	0:30:0	0:15:0	3:0:0

☐ Spray mold with Teflon

☐ Pre-press mold and graphite

Recipe Volume_____

Comments:

8.4 Appendix D: Solidworks Aerogel Sample Holder for Reflectometer

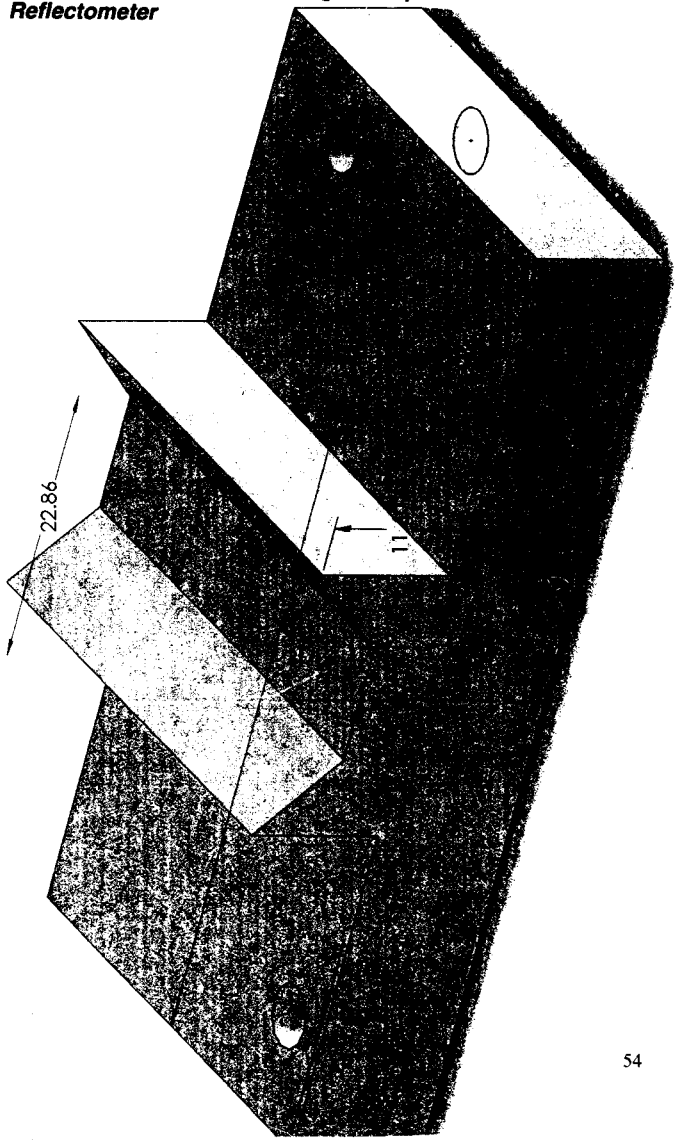

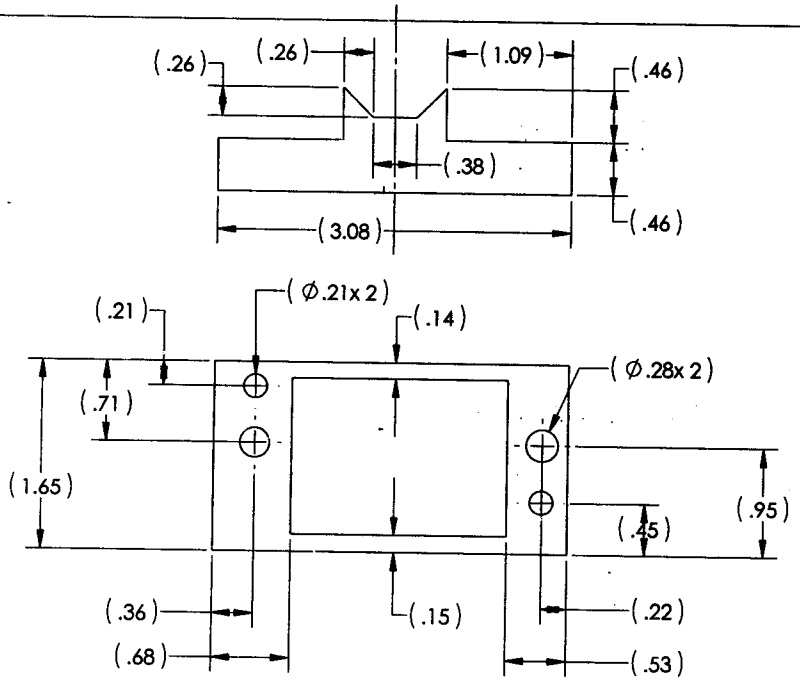

		UNLESS OTHERWISE SPECIFIED:		NAME	DATE
		DIMENSIONS ARE IN INCHES TOLERANCES: FRACTIONAL ± ANGULAR: MACH ± BEND ± TWO PLACE DECIMAL ± THREE PLACE DECIMAL ±	DRAWN		
			CHECKED		
			ENG APPR.		
			MFG APPR.		
		INTERPRET GEOMETRIC TOLERANCING PER:	Q.A.		
		MATERIAL	COMMENTS:		
NEXT ASSY	USED ON	FINISH			
APPLICATION		DO NOT SCALE DRAWING			

TITLE:

SIZE	DWG. NO.	REV
A	shira2	
SCALE: 1:1	WEIGHT:	SHEET 1 OF 1

5 4 3 2 1

8.5 Appendix E: Hot Disk Analyzer Set-Up and Measurement Procedure

The sample holder, also known as the "trapeze," holds the samples and sensor in place and in good contact with one another. The sensor is placed in between two samples; it is used to supply heat to the sample and then record the temperature response of the sample with respect to time. The sensor is connected to the bridge which is used to balance the input and output signals of the sensor. The bridge is connected to the two meters. The source meter is used to control and adjust the power that is supplied to the sensor whereas the purpose of the multimeter is to read the output signal from the sensor, which relates to the temperature of the sample with respect to time. On the computer, the Hot Disk thermal analyzer software records these signals as temperature readings with respect to time and the independent computation system uses this data to calculate the desired measurements including thermal conductivity, specific heat and thermal diffusivity.

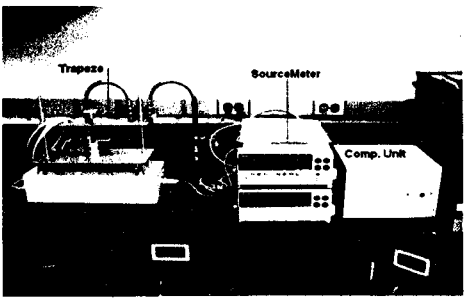

Figure A: Hot Disk Analyzer Set-Up

(http://scoter3.union.edu/~andersoa/AerogelWeb/)

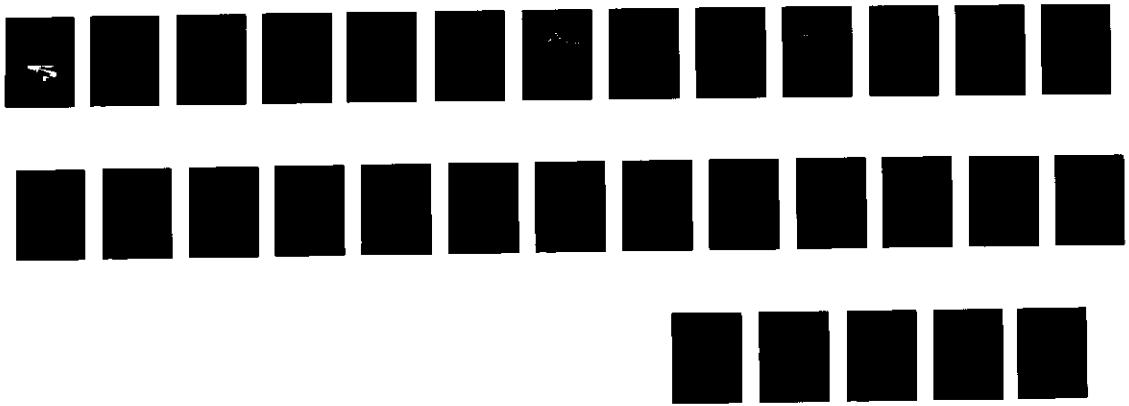

Before performing thermal conductivity measurements with the thermal analyzer, it was important to remember to make sure that all of the equipment had been turned on and left alone for at least an hour in order for the instrument to properly "warm up." If the equipment was not up and running for a sufficient period of time before proceeding with the experiment, the data results provided would not be stable.

For a two-sided test, one aerogel sample was placed on the metal stand with the C5465 sensor in between it and another sample. On the very top of this "sandwich" set-up the small aluminum square plate, was placed to secure the sensor between the two aerogels. If necessary, the sample screw on top of the trapeze or the sensor holder screws were turned to secure each component in place. In this case, the aluminum plate also aided in evenly displacing the load of the top sample screw across the surface of the fragile aerogel sample.

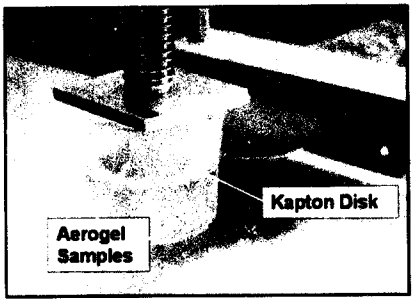

Figure B: Aerogel and Sensor Set-Up in Hot Disk Thermal Analyzer Trapeze

(http://scoter3.union.edu/~andersoa/AerogelWeb/)

When the samples were in place, the computation unit and analysis program were started by clicking on the Hot Disk icon on the desk top. The Keithly Bridge experiment was selected and the appropriate power, sensor, and measurement time parameters were entered on the screen. After the test parameters were set, the sensor had to be balanced using the bridge at the extended range. The marker must be placed within the acceptance region as close to the center (zero on the multimeter) as possible by turning the knob on the bridge. When this was accomplished it was possible to start the measurement. The data was then recorded onto the computer and a file was produced. Before proceeding with the thermal conductivity calculations, the Time vs. Temperature Drift plot was accessed. In order to obtain a reliable analysis, this plot should have no trend. If an observable trend was present the samples were allowed to "cool" in ambient conditions for ten minutes and the test was repeated until the desired results were achieved. Once the plot was inherently random, the file was saved and labeled and the calculations were processed.

A fine-tuned analysis was used with time correction and only a portion of the previous plot. Once the parameters for the calculation were set, the analysis was completed. Once again, if the plot of the Square Root of Time vs. Difference Temperature displayed no apparent trends, the measured thermal properties could be considered reliable and recorded. If the plot has a trend, an apparent increase, decrease or pattern, a different set of points from the Time vs. Temperature Drift plot were chosen. The objective was to use the maximum amount of points possible for the analysis without seeing a trend in the resulting Square Root of Time vs. Difference Temperature plot. If this proved to be unachievable the entire test was rerun until no trend was observed.

8.6 Appendix F: Reflectometer Set-Up and Measurement Procedure

To turn on the system, press the green on/off switch on the left hand side of the reflectometer. This instrument will need approximately 25 minutes to warm up before any measurements can be taken. Next, turn on the computer and the monitor. Open the program by going to the Start menu, clicking on Programs, then PerkinElmer Applications and selecting the Lamda 900 icon. The UV WinLab L800/L900 window will pop-up and automatically display the methods window.

To perform transmittance measurements on an aerogel sample the AEROGEL.MSC method was created. This file is set up to scan each sample using ultraviolet and visible wavelengths of light in the range 200-3000 nm. Press 'Start' to begin taking measurements. The operator is then asked to perform a background correction for a baseline aerogel. The operator should select 'Yes' and will then be prompted to insert the next sample 'blank'. To perform this correction with an air blank, simply close the lid to the spectrometer and click 'Yes'. After the background correction the operator is then prompted to insert the next sample and the program automatically indicates the name of the file to which the data will be saved to. After inserting the appropriate sample and closing the lid the operator should click OK. After the scan is complete, the method will automatically save the data to a notebook file labeled with the initials "SGM" and the test number. The program will then automatically prompt the user to insert the next sample. When the operator is finished taking data and tries to exit the program, the Save Data Window will automatically appear and the data can be saved by selecting 'Save All'. To retrieve the data click on the My Computer icon on the desktop and select the [C:] drive. Then, in the 'UVwinlab' folder click on the 'Data' folder to find

the notebook files holding the data of each spectrum. The data recorded can then be imported into an excel document. The raw data in excel is then analyzed by plotting percent transmittance as a function of wavelength from 200 to 3000 nm. A second plot is made focusing on just the visible region by only plotting wavelengths 300 to 600 nm.

8.7 Appendix G: Fluorometer Set-Up and Measurement Procedure

It is important to set up the instrument in the proper order. The lamp must be ignited first before all other parts of the equipment are powered because it sends a large current through the system which has the potential to damage the other components. To turn on the lamp press the power button. This system has an auto-ignite feature; within one minute the lamp should ignite and the number in the current display should increase until it reads 70 watts. The lamp will need approximately 25 minutes to completely warm up before any measurements can be taken. Next, turn on the power strip in back of the fluorometer. Then flip up the small toggle switch (bottom one) on the back side of the photomultiplier detector (PMT). The voltage display on the PMT should read 1000. Lastly, turn on the computer and its monitor and start the fluorometer program by double clicking on the Felix icon on the desktop. As soon as the program was up and running Open Acquisition was selected.

To control the excitation and emission slit widths rotate the knobs at both ends of each monochromator. There is a marker on the knob to help indicate its position. Because it is difficult to tell what the last operator used, turn the knobs all the way closed and count the rotations from this position. One rotation will open the slit 2 nanometers. It is important to remember that both settings on a single monochromator must be the same but the exitation and emission slits may differ as they are not related to one another.

It is very likely that at the beginning of the session the instrument will indicate that it is having trouble communicating with the Brytebox. In order to fix this problem go to the box behind the printer; there should be a red light, under which there is a toggle

switch. Turn off the box using the switch, wait approximately 30 seconds and turn it back on. The light will probably be red at first and then switch green. If this does not solve the problem call Mary Carroll for further assistance.

While performing emission and time-based scans on the aerogel samples, make sure the monochromator's excitation and emission wavelengths are calibrated correctly. Also, the excitation of a sample should never be within the emission range.

To turn on the nitrogen tank, only a small turn of the main knob is necessary to do so. The nitrogen flow from the tank can then be further and more precisely controlled by the left-hand side of the gas proportioner. To increase the flow to the cuvette the left knob on the gas proportioner should be turned to the left. In order to measure the flow of nitrogen to the cuvette both the level of the stainless steel (silver color) and carboloy (black color) ball must be recorded and compared to the conversion chart located in the drawer beneath the system's computer monitor labeled "Flowmeter Calibration Data".

8.8 Appendix H: Emission Spectra of PtOEP-Doped Aerogels in 100% Nitrogen

All fluorescence spectra were taken at an excitation wavelength of 533 nm using 2 nm slit widths for both excitation and emission monochromators.

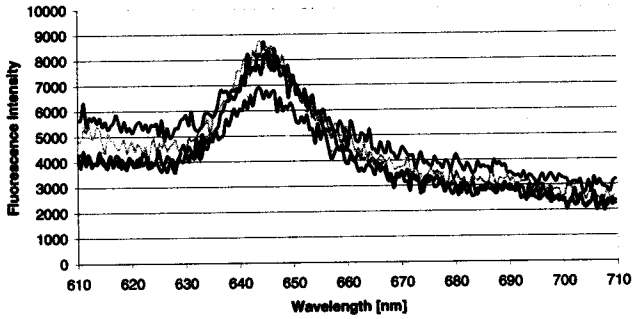

Figure A: Fluorescence of PtOEP-Doped Aerogel Sample (50% Increase in Water)

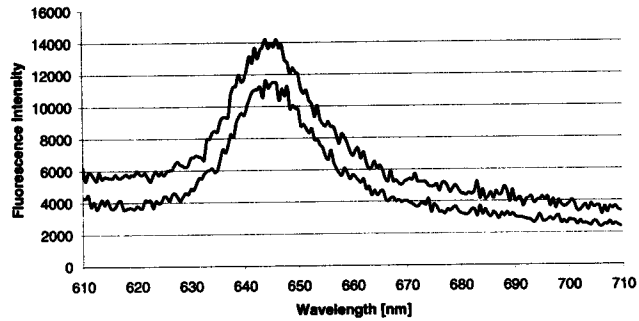

Figure B: Fluorescence of PtOEP-Doped Aerogel Sample (50% Increase in Water from Second Sample)

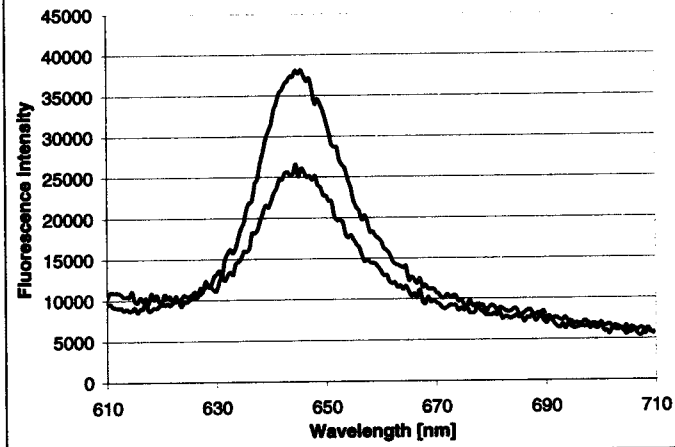

Figure C: Fluorescence of PtOEP-Doped Aerogel Sample (25% Increase in Water)

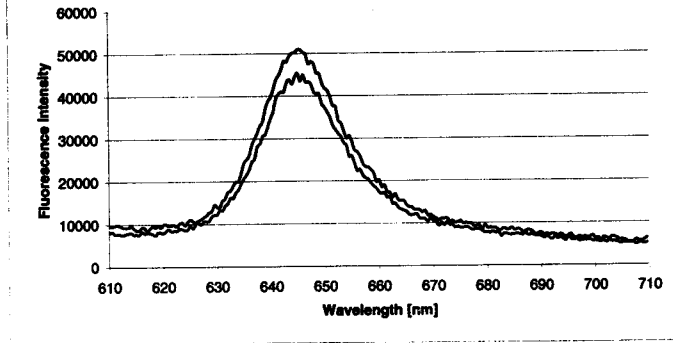

Figure D: Fluorescence of PtOEP-Doped Aerogel Sample
(25% Increase in Water from Second Sample)

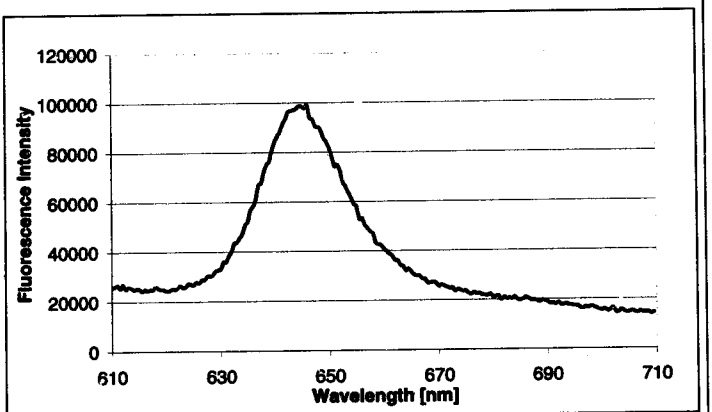

Figure E: Fluorescence of PtOEP-Doped Aerogel Sample (Standard Recipe)

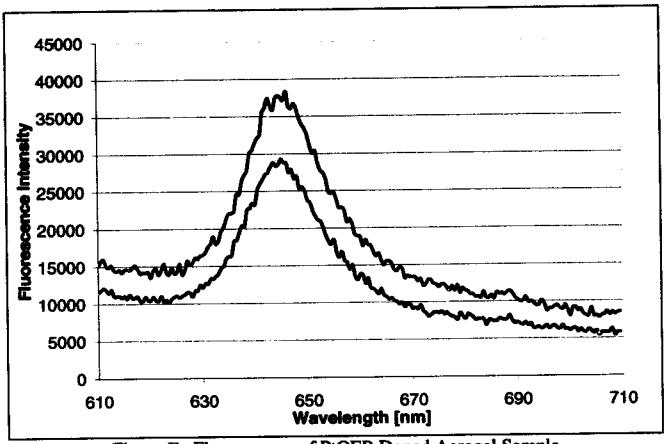

Figure F: Fluorescence of PtOEP-Doped Aerogel Sample
(Standard Recipe from Second Sample)

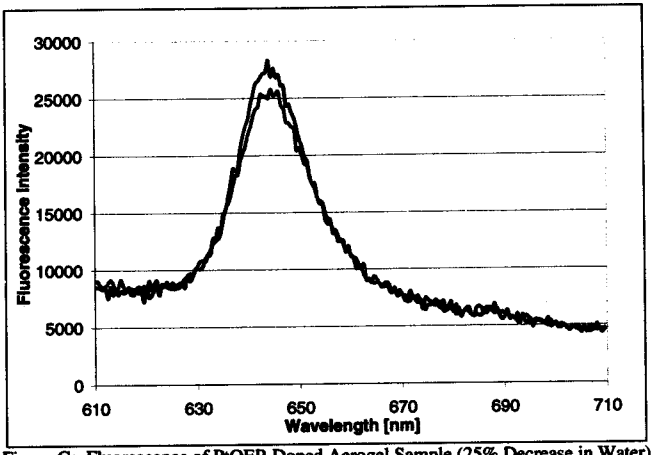

Figure G: Fluorescence of PtOEP-Doped Aerogel Sample (25% Decrease in Water)

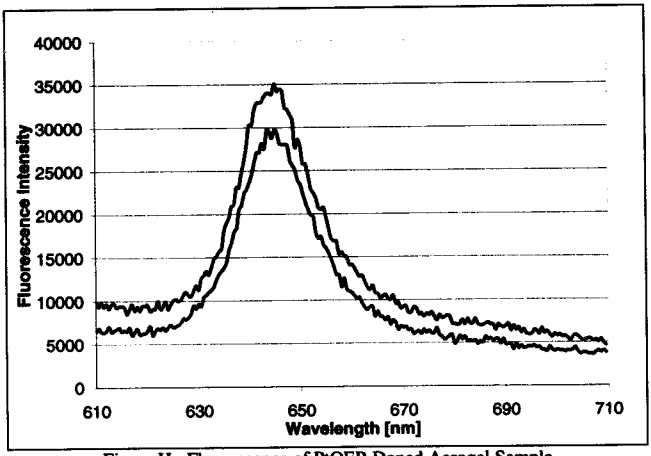

Figure H: Fluorescence of PtOEP-Doped Aerogel Sample
(25% Decrease in Water from Second Sample)

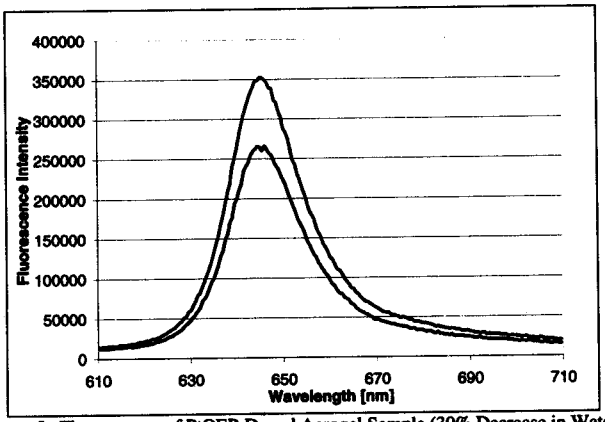

Figure I: Fluorescence of PtOEP-Doped Aerogel Sample (30% Decrease in Water)

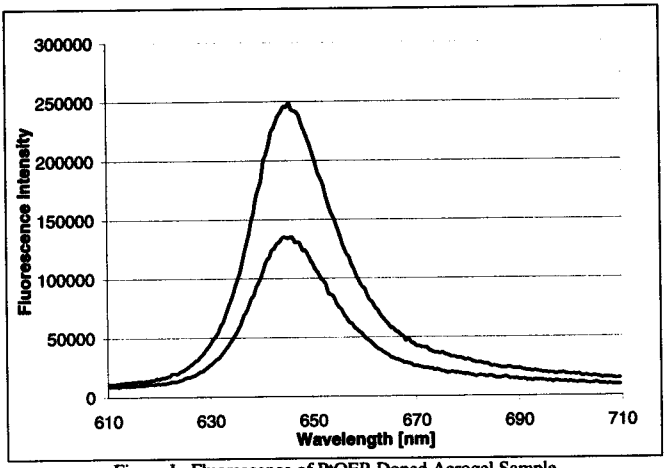

Figure J: Fluorescence of PtOEP-Doped Aerogel Sample
(30% Decrease in Water from Second Sample)

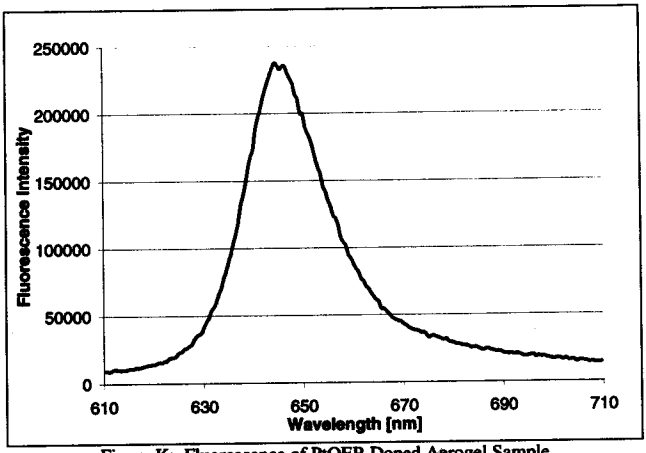

Figure K: Fluorescence of PtOEP-Doped Aerogel Sample
(30% Decrease in Water from Third Sample)

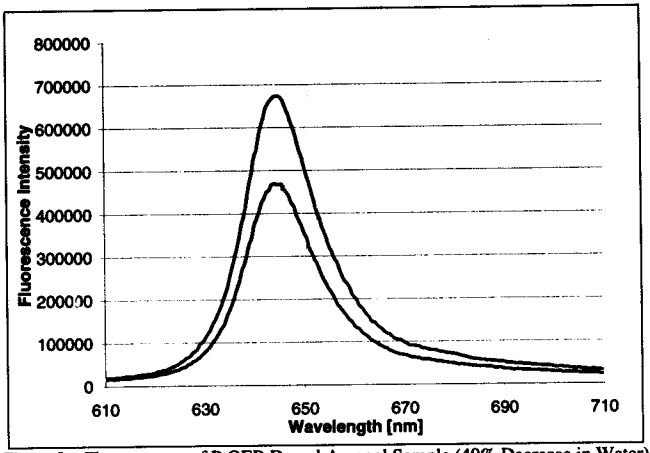

Figure L: Fluorescence of PtOEP-Doped Aerogel Sample (40% Decrease in Water)

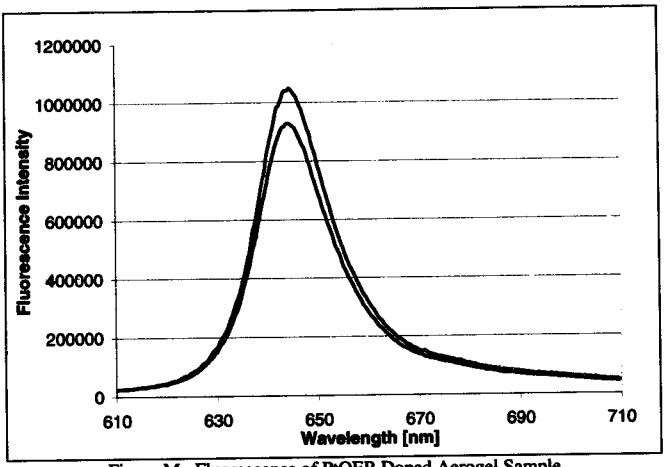

Figure M: Fluorescence of PtOEP-Doped Aerogel Sample
(40% Decrease in Water from Second Sample)

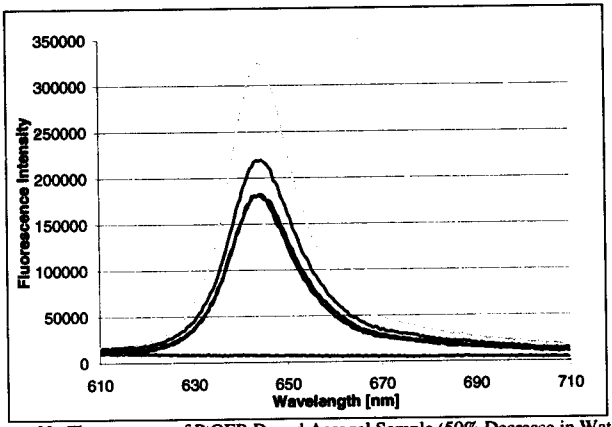

Figure N: Fluorescence of PtOEP-Doped Aerogel Sample (50% Decrease in Water)

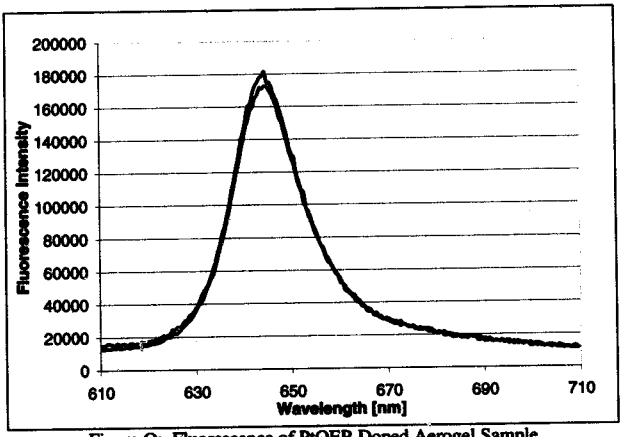

Figure O: Fluorescence of PtOEP-Doped Aerogel Sample
(50% Decrease in Water from Second Sample)

8.9 Appendix I: $F_{(100\% N2)}/F_{(Air)}$ for Each PtOEP-Doped Aerogel

Table A: Raw Data of $F_{(100\% N2)}/F_{(Air)}$ for Each PtOEP Doped Aerogel Sample

	Fair	Fnitrogen	Fair/Fnitrogen
- 50%	$7.52 \times 10^{+3}$	$1.70 \times 10^{+5}$	22.7
- 50% (2)	$1.03 \times 10^{+4}$	$2.58 \times 10^{+5}$	25.0
- 50% (2)	$8.77 \times 10^{+3}$	$2.07 \times 10^{+5}$	23.6
- 50%	$9.40 \times 10^{+3}$	$1.67 \times 10^{+5}$	17.9
- 50% (2)	$7.95 \times 10^{+3}$	$1.65 \times 10^{+5}$	20.8
- 25%	$5.81 \times 10^{+3}$	$2.64 \times 10^{+4}$	4.5
- 25%	$5.85 \times 10^{+3}$	$2.46 \times 10^{+4}$	4.2
- 25%	$6.33 \times 10^{+3}$	$3.27 \times 10^{+4}$	5.2
- 25% (2)	$4.30 \times 10^{+3}$	$2.78 \times 10^{+4}$	6.5
Standard	$1.96 \times 10^{+4}$	$9.08 \times 10^{+4}$	4.6
Standard	$9.77 \times 10^{+3}$	$3.16 \times 10^{+4}$	3.2
Standard	$1.15 \times 10^{+4}$	$3.72 \times 10^{+4}$	3.2
+ 25%	$8.41 \times 10^{+3}$	$3.63 \times 10^{+4}$	4.3
+ 25%	$8.81 \times 10^{+3}$	$2.57 \times 10^{+4}$	2.9
+ 25%	$6.84 \times 10^{+3}$	$4.78 \times 10^{+4}$	7.0
+ 25% (2)	$5.99 \times 10^{+3}$	$4.45 \times 10^{+4}$	7.4
+ 50%	$3.61 \times 10^{+3}$	$7.56 \times 10^{+3}$	2.1
+ 50%	$4.40 \times 10^{+3}$	$7.58 \times 10^{+3}$	1.7
+ 50% (2)	$3.01 \times 10^{+3}$	$7.24 \times 10^{+3}$	2.4
+ 50% (2)	$3.21 \times 10^{+3}$	$6.54 \times 10^{+3}$	2.0
+ 50%	$4.69 \times 10^{+3}$	$1.30 \times 10^{+4}$	2.8
+ 50% (2)	$3.16 \times 10^{+3}$	$1.10 \times 10^{+4}$	3.5

*(2) indicates that the aerogel is from the second sample.

8.10 Appendix J: Time-based Scans of PtOEP-Doped Aerogels

Figure A: Time-Based Scan of PtOEP-Doped Aerogel (+50% Water) at 646 nm

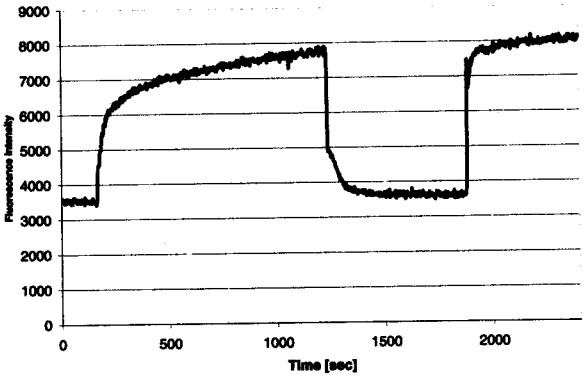

Figure B: Time-Based Scan of PtOEP-Doped Aerogel (+50% Water) at 646 nm

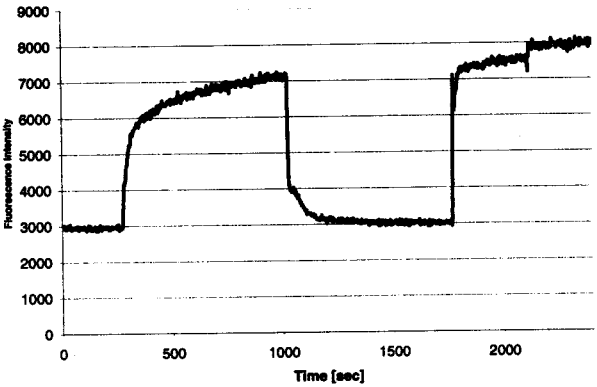

Figure C: Time-Based Scan of PtOEP-Doped Aerogel (+ 50% H_2O) at 646 nm

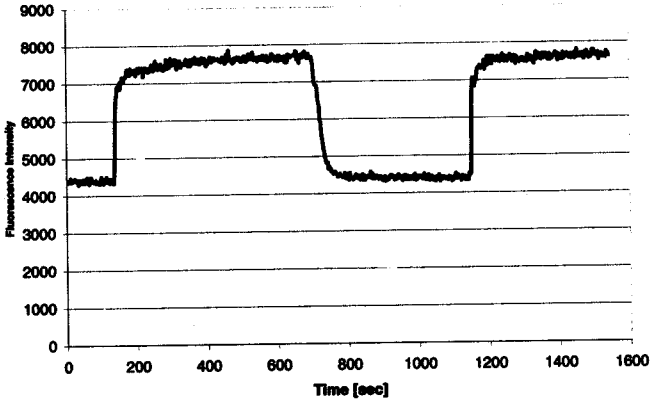

Figure D: Time-Based Scan of PtOEP-Doped Aerogel (+ 50% H_2O) at 646 nm

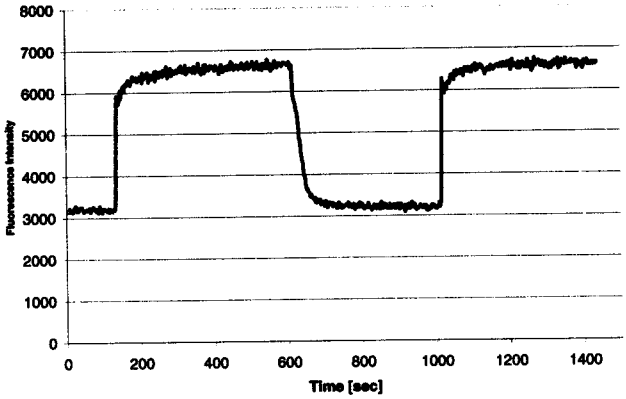

Figure E: Time-Based Scan of PtOEP-Doped Aerogel (+ 50% H_2O) at 646 nm

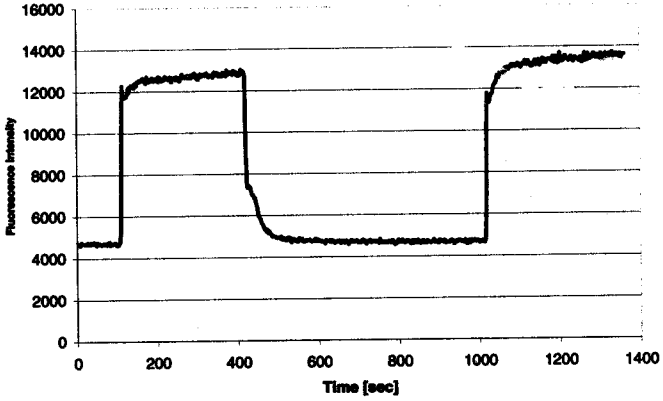

Figure F: Time-Based Scan of PtOEP-Doped Aerogel (+ 50% H_2O) at 646 nm

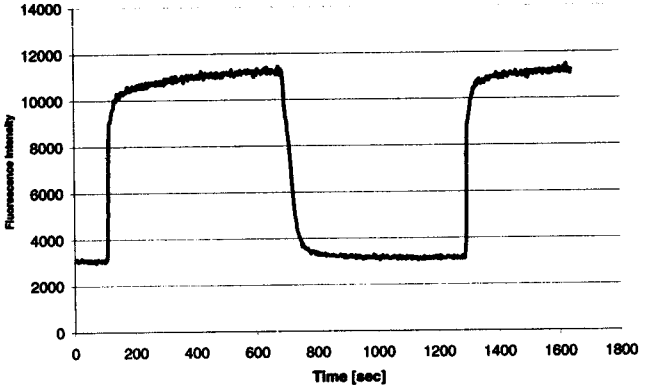

Figure G: Time-Based Scan of PtOEP-Doped Aerogel (+25% Water) at 646 nm

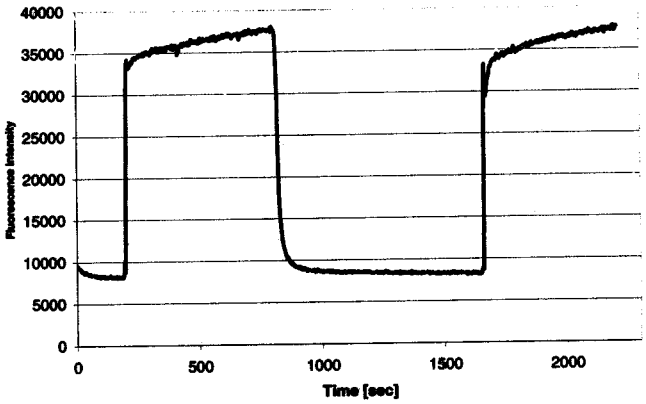

Figure H: Time-Based Scan of PtOEP-Doped Aerogel (+ 25% H_2O) at 646 nm

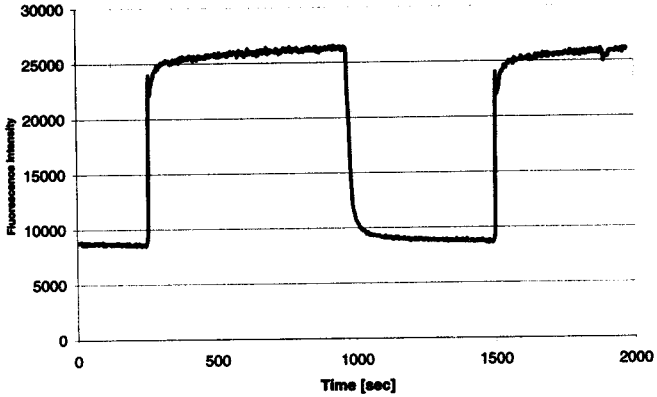

Figure I: Time-Based Scan of PtOEP-Doped Aerogel (+ 25% H_2O) at 646 nm

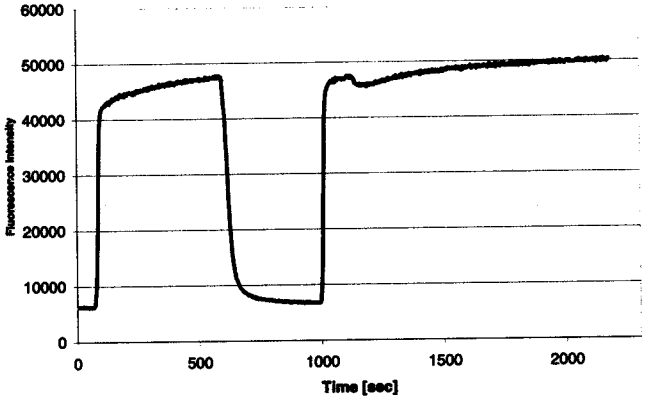

Figure J: Time-Based Scan of PtOEP-Doped Aerogel (+ 25% H_2O) at 646 nm

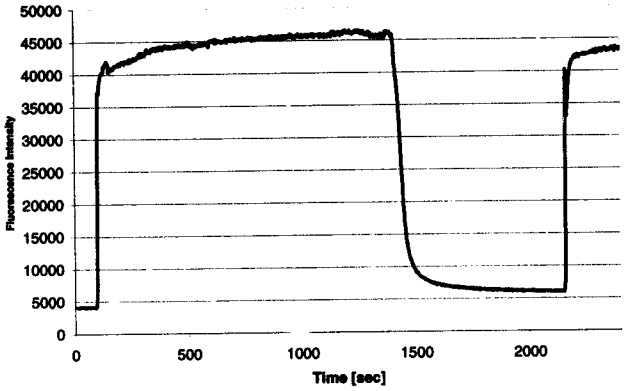

Figure K: Time-Based Scan of PtOEP-Doped Aerogel (Standard) at 646 nm

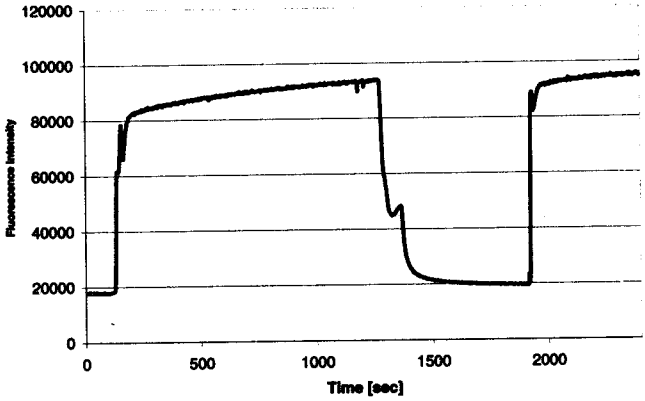

Figure L: Time-Based Scan of PtOEP-Doped Aerogel (Standard) at 646 nm

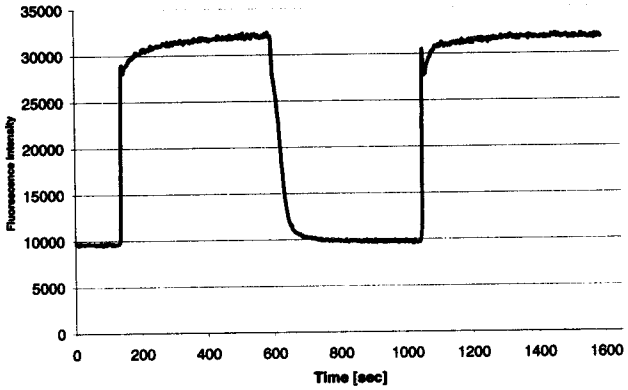

Figure M: Time-Based Scan of PtOEP-Doped Aerogel (Standard) at 646 nm

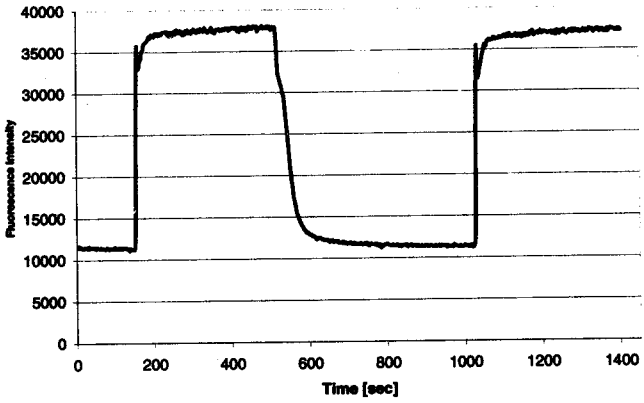

Figure N: Time-Based Scan of PtOEP-Doped Aerogel (- 25% H_2O) at 646 nm

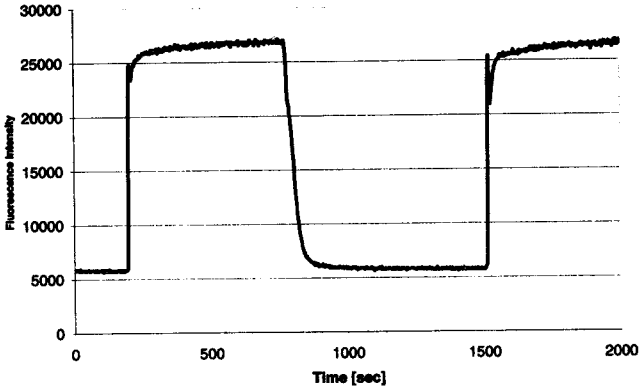

Figure O: Time-Based Scan of PtOEP-Doped Aerogel (- 25% H_20) at 646 nm

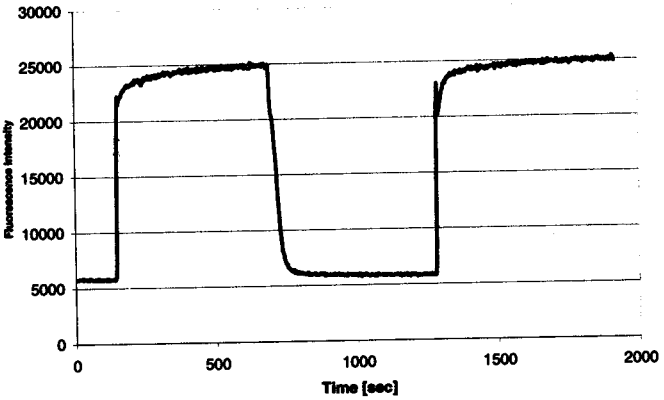

Figure P: Time-Based Scan of PtOEP-Doped Aerogel (- 25% H_20) at 646 nm

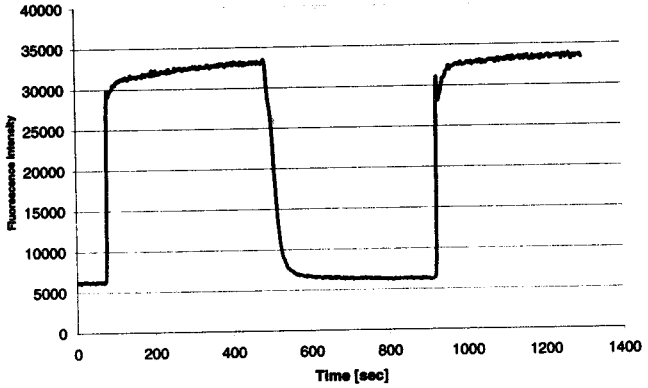

Figure Q: Time- Based Scan of PtOEP-Doped Aerogel (- 25% H_2O) at 646 nm

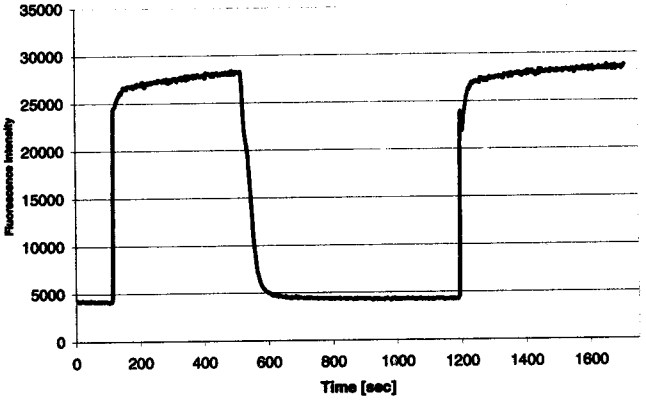

Figure R: Time-Based Scan of PtOEP-Doped Aerogel (-30% Water) at 646 nm

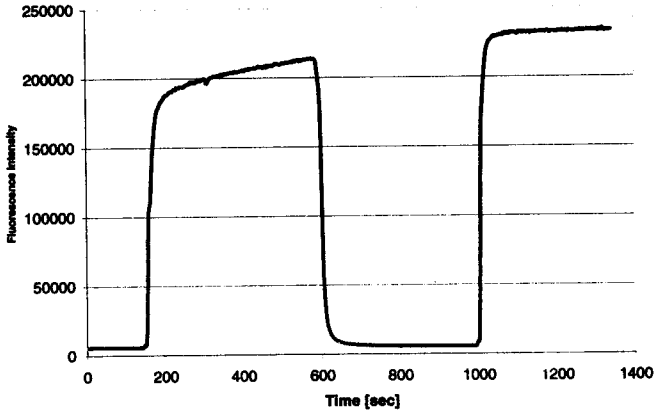

Figure S: Time-Based Scan of PtOEP-Doped Aerogel (-30% Water) at 646 nm

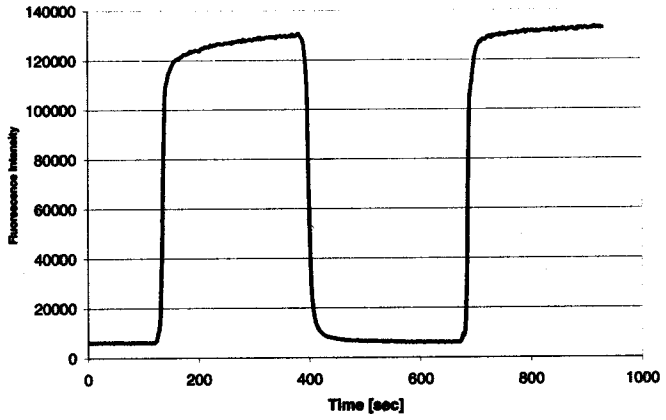

Figure T: Time-Based Scan of PtOEP-Doped Aerogel (-30% Water) at 646 nm

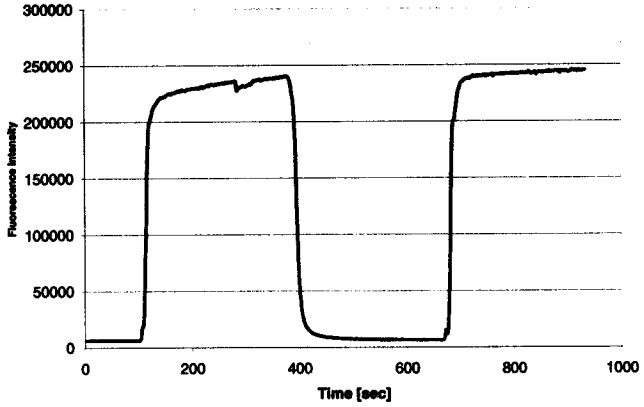

Figure U: Time-Based Scan of PtOEP-Doped Aerogel (~30% Water) at 646 nm

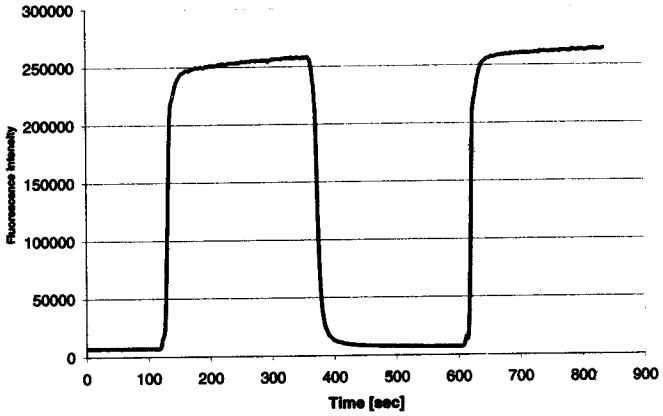

Figure V: Time-Based Scan of PtOEP-Doped Aerogel (~30% Water) at 646 nm

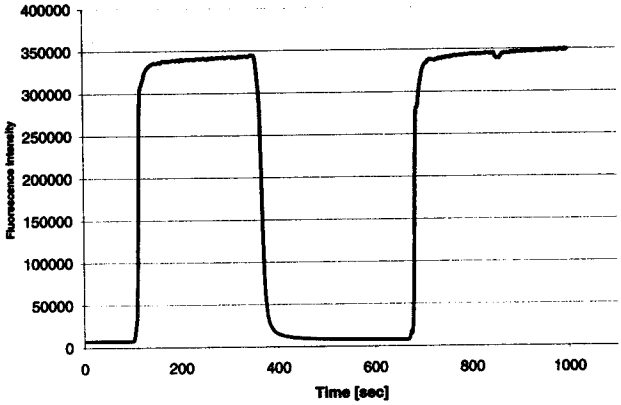

Figure W: Time-Based Scan of PtOEP-Doped Aerogel (~40% Water) at 646 nm

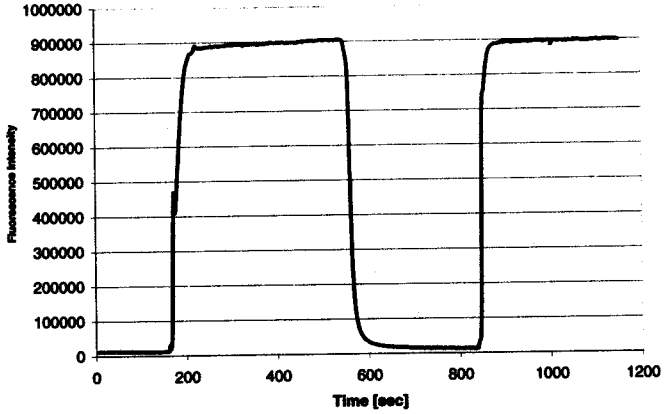

Figure X: Time-Based Scan of PtOEP-Doped Aerogel (~40% Water) at 646 nm

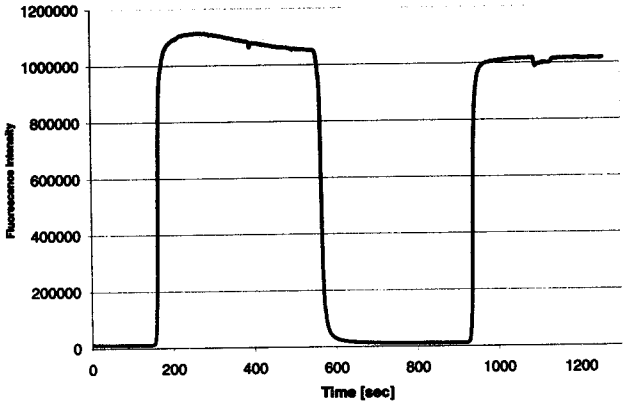

Figure Y: Time-Based Scan of PtOEP-Doped Aerogel (-40% Water) at 646 nm

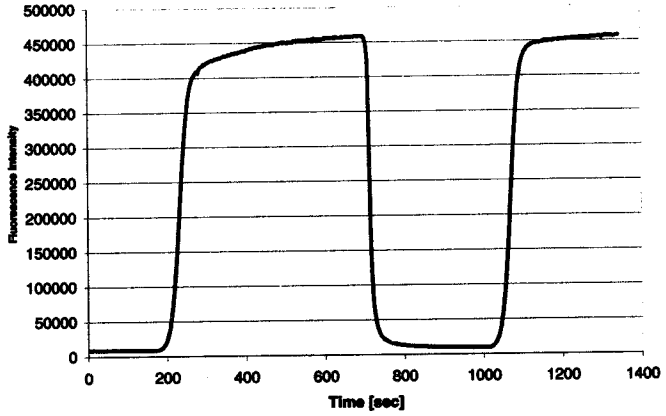

Figure Z: Time-Based Scan of PtOEP-Doped Aerogel (-40% Water) at 646 nm

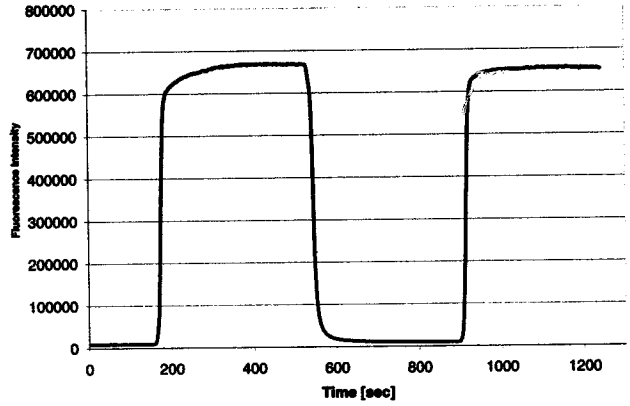

Figure AA: Time-Based Scan of PtOEP-Doped Aerogel (- 50% H_2O) at 646 nm

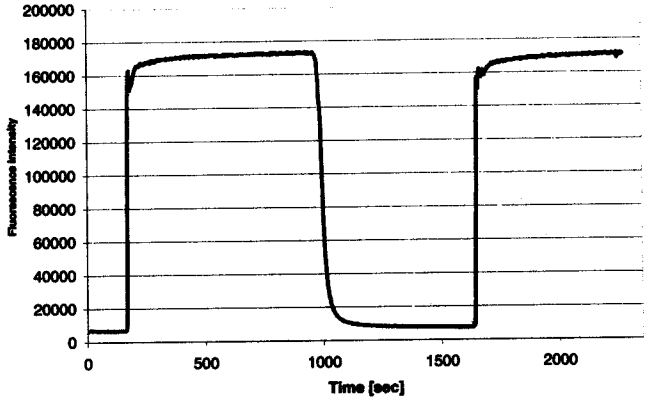

Figure AB: Time-Based Scan of PtOEP-Doped Aerogel (- 50% H_2O) at 646 nm

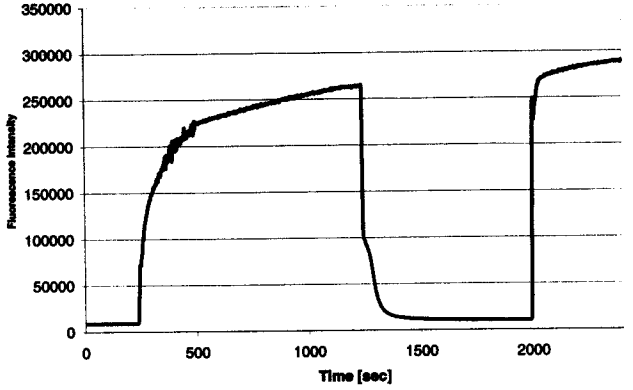

Figure AC: Time-Based Scan of PtOEP-Doped Aerogel (- 50% H_2O) at 646 nm

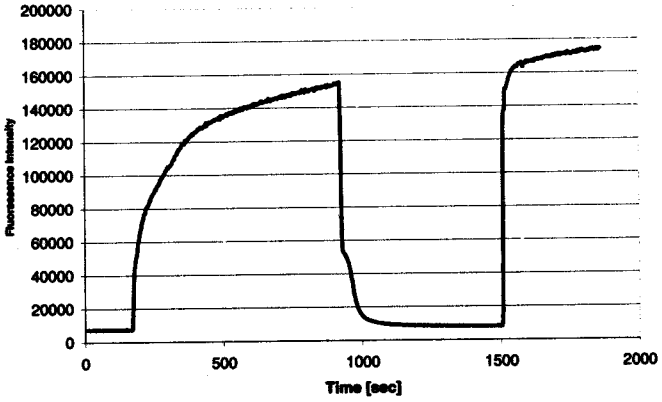

Figure AD: Time-Based Scan of PtOEP-Doped Aerogel (- 50% H_2O) at 646 nm

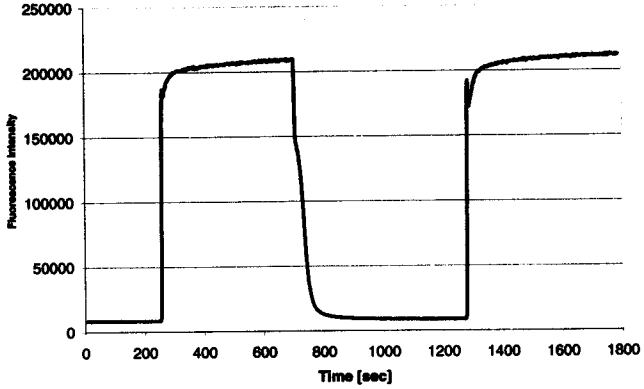

Figure AE: Time-Based Scan of PtOEP-Doped Aerogel (- 50% H_2O) at 646 nm

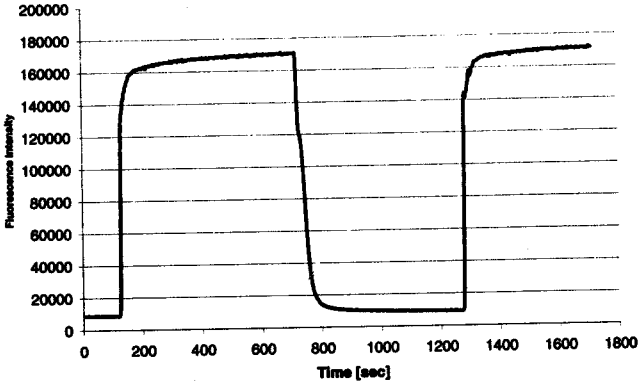

Figure AF: Time-Based Scan of PtOEP-Doped Aerogel (- 50% H_2O) at 646 nm